Predicting High-Lift Aerodynamics on NASA Common Research Model

Part-III: Wall-Modeled Large Eddy Simulations

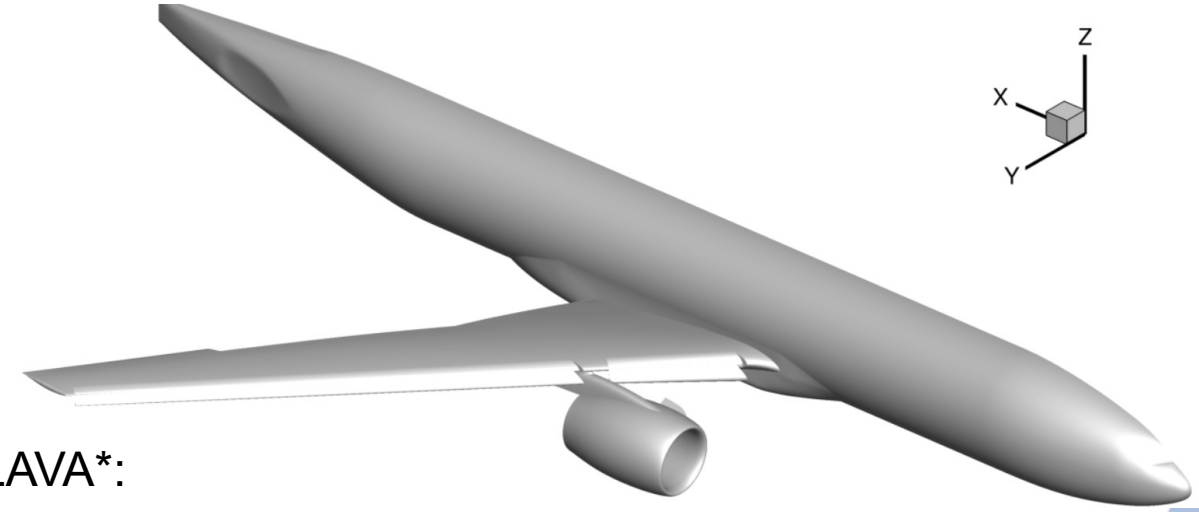
Aditya S. Ghate, Gaetan K.W. Kenway, Gerrit-Daniel Stich, Daniel Maldonado, Cetin C. Kiris

Computational Aerosciences Branch
NASA Ames Research Center

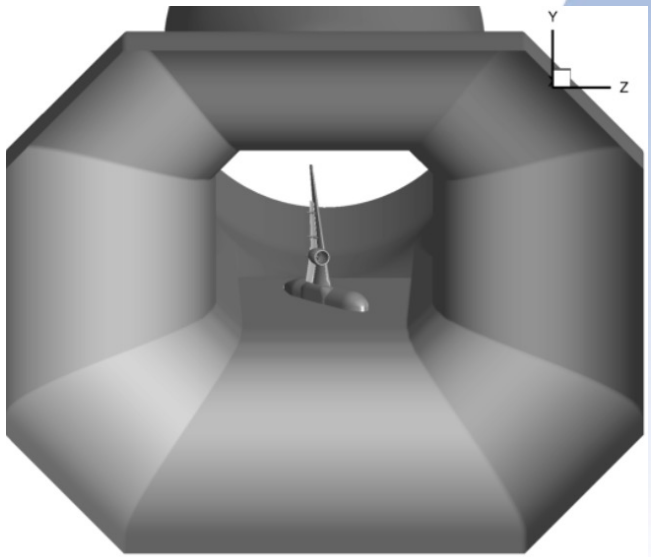
Advanced Modeling and Simulation (AMS) Seminar Series
NASA Ames Research Center, June 9th 2022

NASA High-Lift Common Research Model

- HL-CRM tested in QinetiQ tunnel (Farnborough, UK) **(Evans et al., 2020)** at:
  - $\mathrm{Re}_{\mathrm{MAC}} = 5.5\times10^{6}$
  - $\mathrm{M}_{\mathrm{REF}} = 0.2$
- HLPW4 Case 2a and Case 2b



- 3 distinct turbulence closure methods studied using LAVA*:
  - RANS (Curvilinear Overset grids)
  - DDES (Curvilinear Overset grids)
  - **WMLES (Curvilinear Overset grids and Cartesian Octree grids)**
- 4 conference papers (1 at Scitech 2022, 3 at Aviation 2022)



*** Launch, Ascent, and Vehicle Aerodynamics (LAVA)**

Recap - Delayed Detached Eddy Simulations (DDES)

Improves Reynolds Stress Closure by relying on resolved component when the RANS closure fails:

- Across a RANS/LES interface (typically 2-3 grid points; and assuming a "perfect" indicator function)

$$\tau_{ij} \approx -2\nu_{RANS}S_{ij} \approx \tilde{u}_i\tilde{u}_j - 2\nu_{LES}S_{ij}$$

- Consistent utilization requires generation of fluctuations immediately to compensate for the lost modelled stress
- Works great **for bluff-bodies/shear layers**, likely due to presence of inflection points, leading to inertial instabilities generating fluctuations quickly
- Unclear whether advantages translate to **boundary-layer separation**: If there are improvements, do they result due to more accurate Reynolds stress or just reduction of eddy viscosity?
- Zonal methods using synthetic turbulence could potentially address this uncertainty (but might not easily scale to complex geometries)
- However, …

Recap - Delayed Detached Eddy Simulations (DDES)

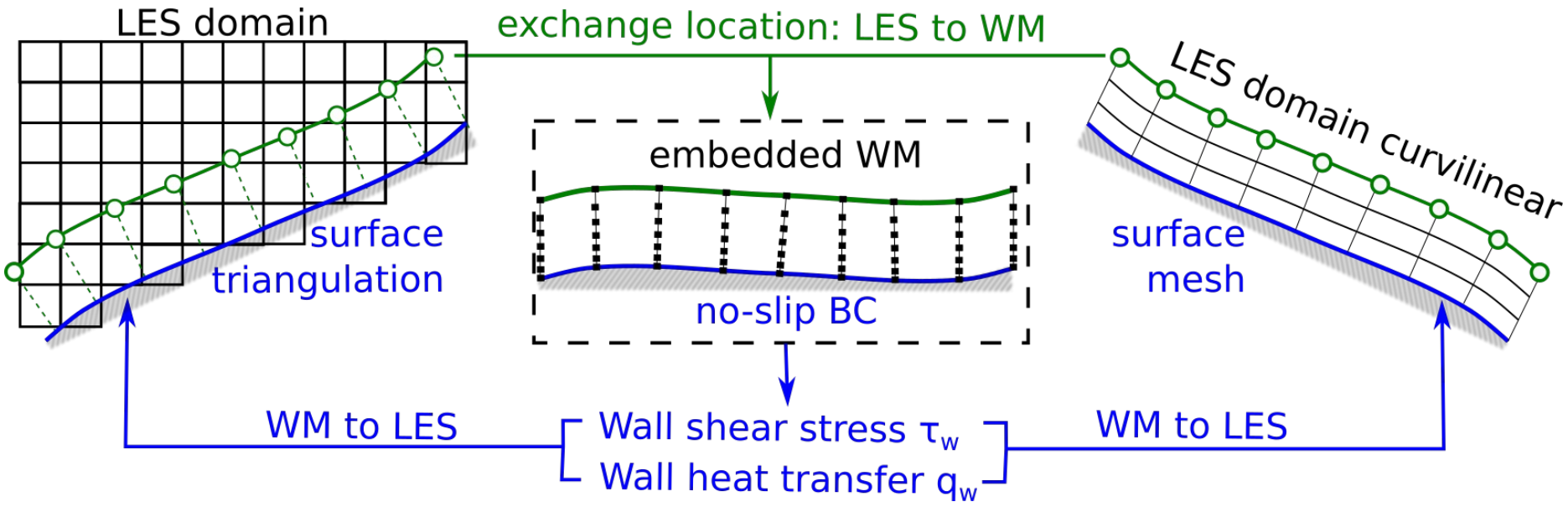
LAVA – DDES does show striking agreement to experiment if the following criteria are met:

- **Sufficient spanwise/streamwise spacing**: Both wing-root and outboard main-element refined substantially over the finest RANS grid that was studied
- **LES-appropriate grids utilized for shear-layers**: Slat wake/main-element wakes require low-aspect ratio grids for resolvable content
- **Low time-step size**: Dissipation due to BDF2 needs to be limited by respecting temporal time-scales corresponding to resolvable length scales $\left(\tau \propto k_{\Delta}^{-\frac{2}{3}}\right)$
- **Low-dissipation discretization**: Convective flux operators need to be non-dissipative
- Sensitivity to underlying RANS closure reduced when **more domain was under LES mode**

➢ DDES solution quality improves as best-practices become more “LES-friendly”

Why not perform LES everywhere and model what is not-resolvable (or subgrid)?

Wall-Modelled Large Eddy Simulations



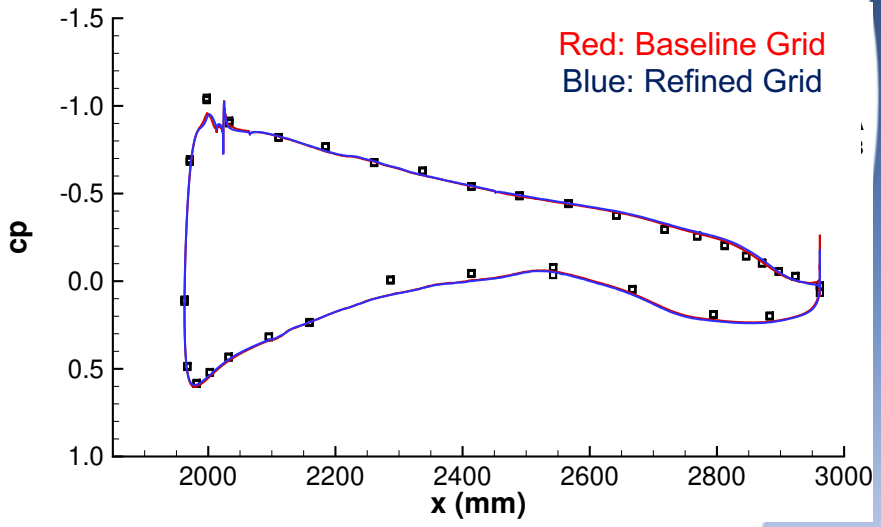
- **Eliminating $y^+ < 1$ constraint** allows for significantly higher streamwise and spanwise resolution for the same computational cost
- Inner-layer (viscous) scales in BL modelled using a **stress-equilibrium assumption**
- Subgrid (subfilter) scales modelled using an **eddy viscosity (dissipative) closure** with some basic properties
- At least **3 potential issues** pertinent to HL-CRM need to be considered:

Wall-Modelled Large Eddy Simulations

Issue 1: How is LES a feasible tool if “grid convergence” requires DNS?

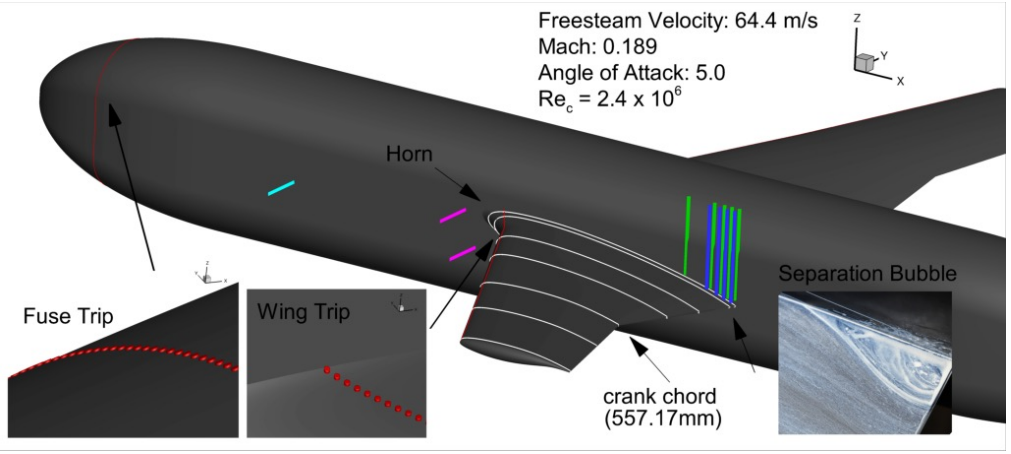
- Meyers & Sagaut (2007) demonstrated non-monotonic convergence of velocity profile for channel flow even for WRLES
- Evidence suggests:
  - Pressure convergences much earlier than velocity profiles (Juncture Flow WMLES)
  - Aerodynamic loads could potentially be obtained within engineering tolerance if “flow topology” is predicted with “adequate accuracy”
- Outcomes of CTR 2018 Summer program (Lehmkuhl et al’s CLmax study) very encouraging

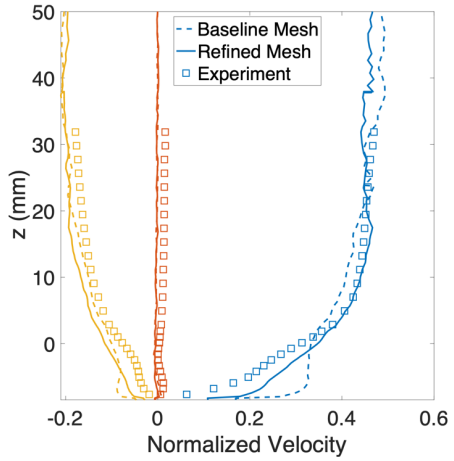
Juncture flow WMLES

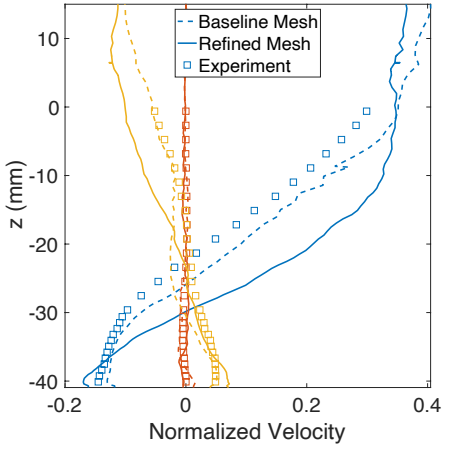


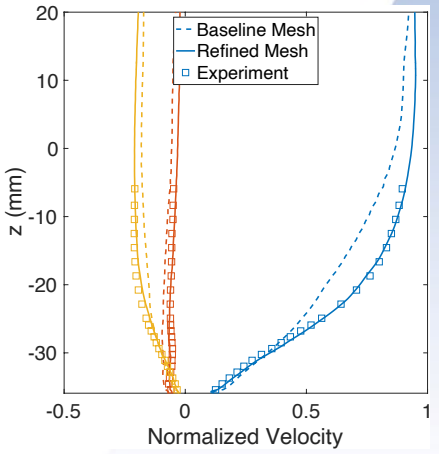
Downstream into the corner-flow bubble

Outboard away from root









Wall-Modelled Large Eddy Simulations

Issue 2: How can equilibrium models predict non-equilibrium flows?

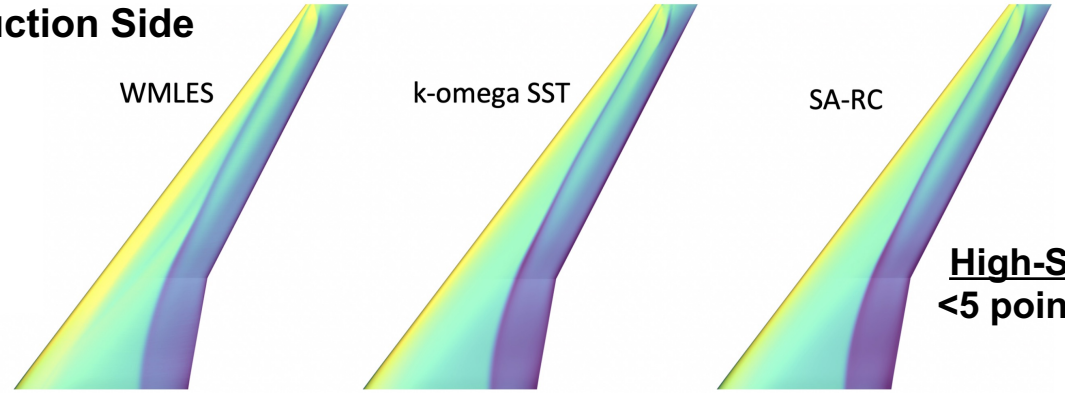
- Coleman et al. (2015) argued for **weak-influence of pressure gradient**
- Main arguments in support of equilibrium modelling:
  - Inner-layer dynamics are much **faster time-scale** than outer-layer dynamics $\left(\tau \propto \frac{k}{\varepsilon}\right)$
  - **Convection and pressure gradient in-balance** at $y^+ > 30$ (Hickel et al., 2012): Need to resolve outer-layer non-equilibrium dynamics (low-dissipation, low-grid AR to prevent artificial geometric anisotropy)
  - Errors due to equilibrium modeling show up **most prominently in skin-friction and not in pressure** – but in these situations skin-friction is close to zero anyway (see Park, 2017)
  - Many of the proposed non-equilibrium models are either: a) **inconsistent**, or b) Not easily scalable to complex geometries
- Equilibrium WMLES grid requirements for **smooth-body separation** remains a topic of research
  - Gaussian bump WMLES are worrying – large grid requirements to predict separation accurately; sensitivity reported to subgrid scale closures (Iyer & Malik, 2021; Agarwal et al., 2022)
  - Incipient separation particularly challenging – could be interpreted as error in angle-of-attack in problems such as HL-CRM

Wall-Modelled Large Eddy Simulations

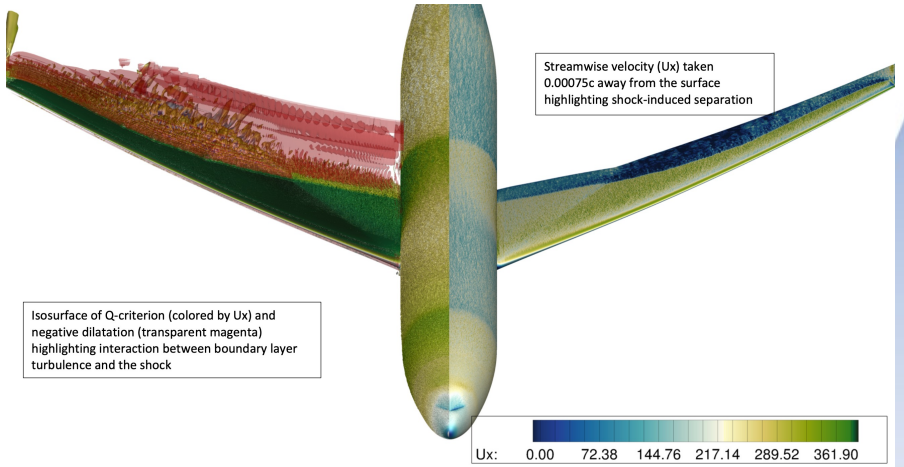
Issue 3: Resolution needed to resolve thin LE boundary layers is a show-stopper.

- Equilibrium attached boundary layers can be predicted correctly with very coarse-grids (4-5 points per δ) : cross-component of Reynolds stresses ($\propto k_{\Delta}^{-7/3}$) correct on coarse grids unlike variances ($\propto k_{\Delta}^{-5/3}$)
- Evidence suggests that errors damp (as opposed to grow) in favorable pressure gradients: Large errors near leading edge do not significantly propagate downstream
- WMLES on coarse grids seem to predict skin-friction drag accurately (compared to RANS on $y^+ < 1$ grids)

Suction Side



<u>High-Speed CRM wing</u>
<5 points per δ at 10%c
$y^+ > 80$



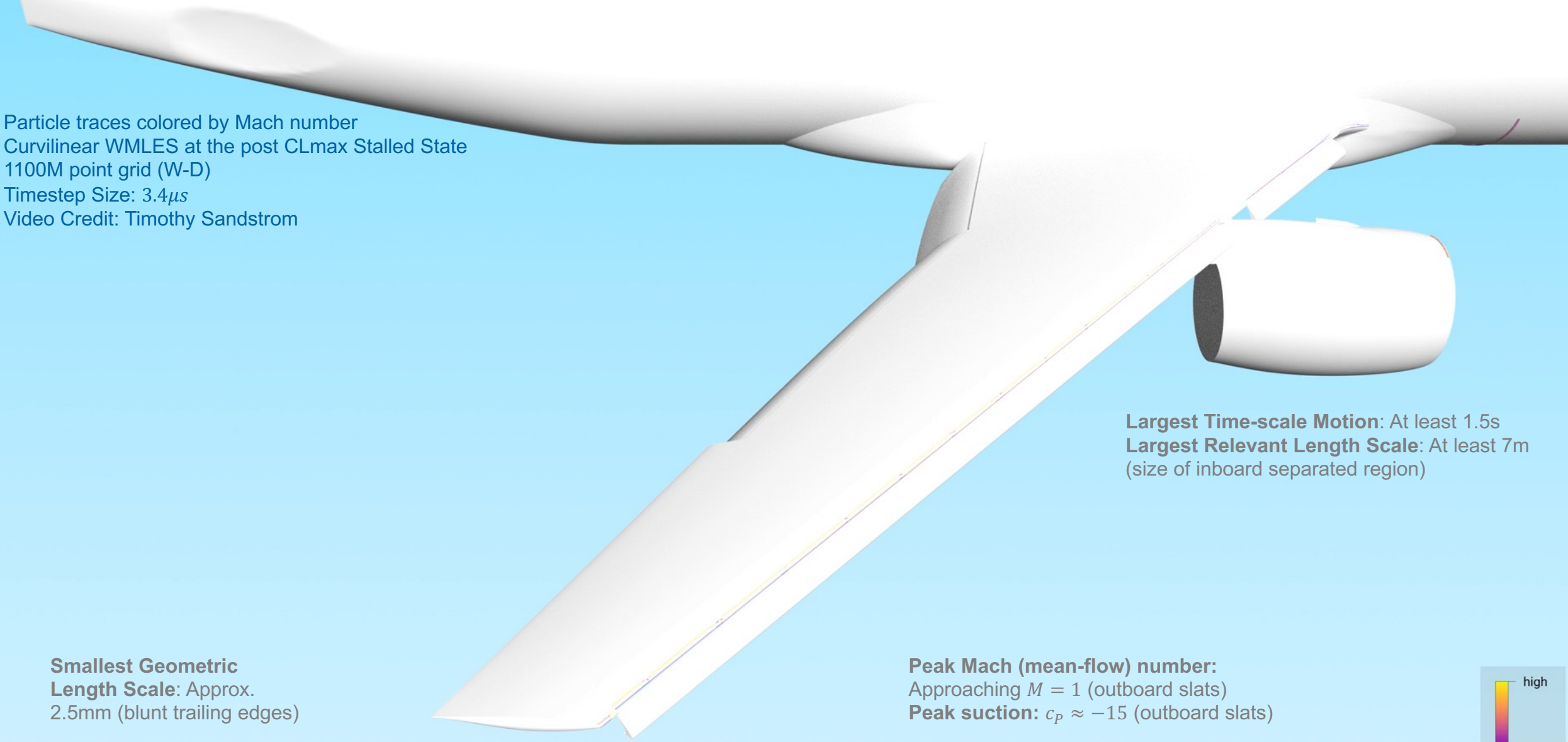
- Thin-BLs are likely to be more problematic when they separate: incorrect variance due to coarse-resolution will affect separation prediction – potential cause for concern on outboard portions of the wing (at high-angles of attack), as well as on the flap (shallow separation at low angles of attack)

Outline

- Grid generation: Curvilinear Overset & Cartesian Octree formulations within LAVA
- Part A: WMLES of the In-Tunnel Configuration
- Part B: Some unexpected results:
  - Onset of stall in free air - differences between Curvilinear and Cartesian WMLES
  - Onset of stall in tunnel - Inviscid tunnel walls vs Viscous tunnel walls
- Part C: Numerical experiments to understand uncertainties with Free-Air corrections
- Computational costs and outlook
- Summary

The Flow: CRM-HL at the stalled state

Particle traces colored by Mach number
Curvilinear WMLES at the post CLmax Stalled State
1100M point grid (W-D)
Timestep Size: $3.4\mu s$
Video Credit: Timothy Sandstrom

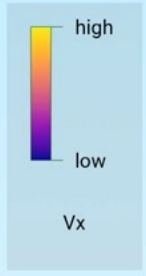


Largest Time-scale Motion: At least 1.5s
Largest Relevant Length Scale: At least 7m
(size of inboard separated region)

Smallest Geometric Length Scale: Approx. 2.5mm (blunt trailing edges)

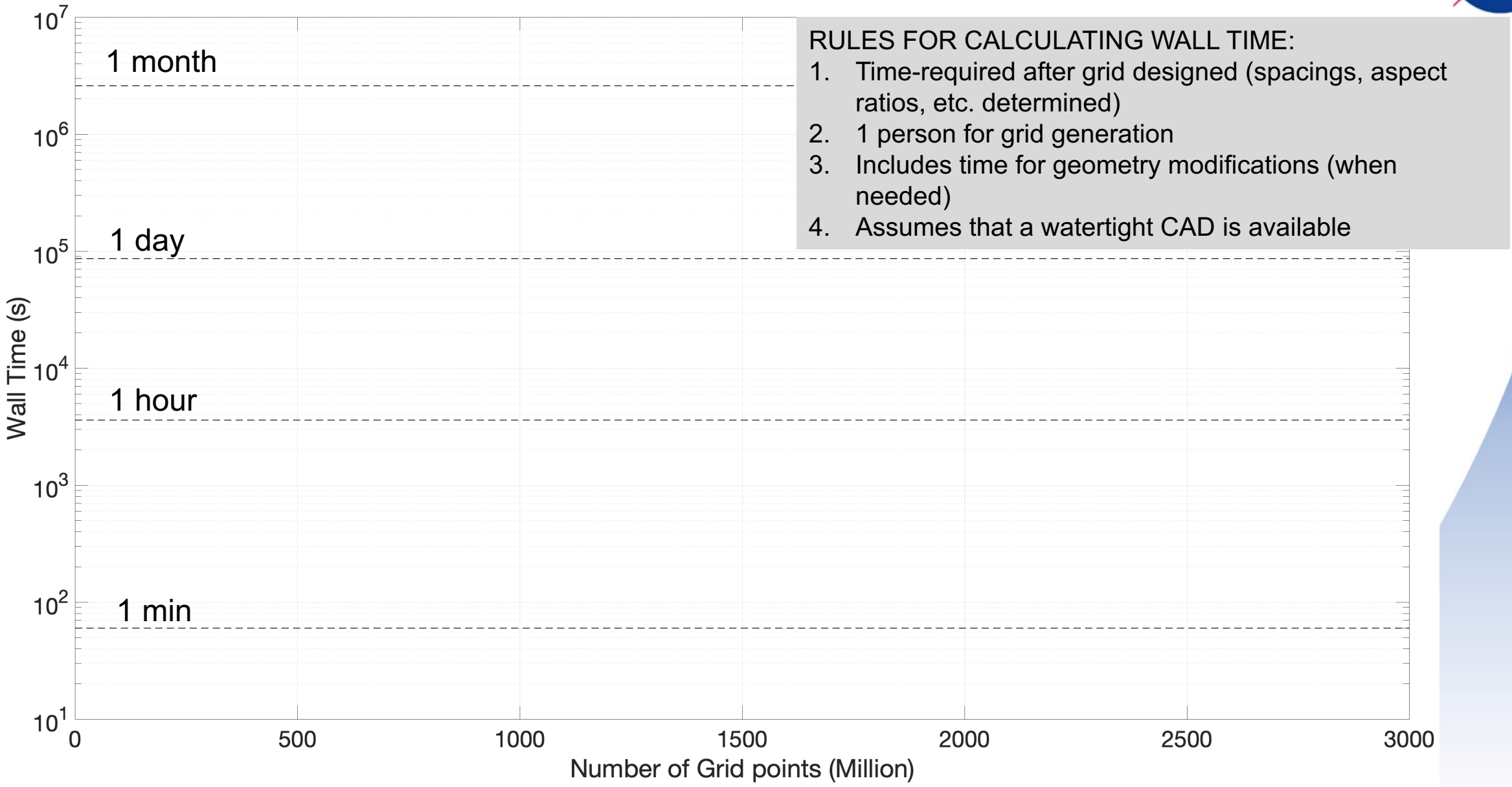
Fastest Time-scale Motion: Approx. $600\ \mu s$
(shedding time-scale for slat brackets)

Peak Mach (mean-flow) number:
Approaching $M = 1$ (outboard slats)
Peak suction: $c_P \approx -15$ (outboard slats)



Grid Generation and Numerical Algorithms

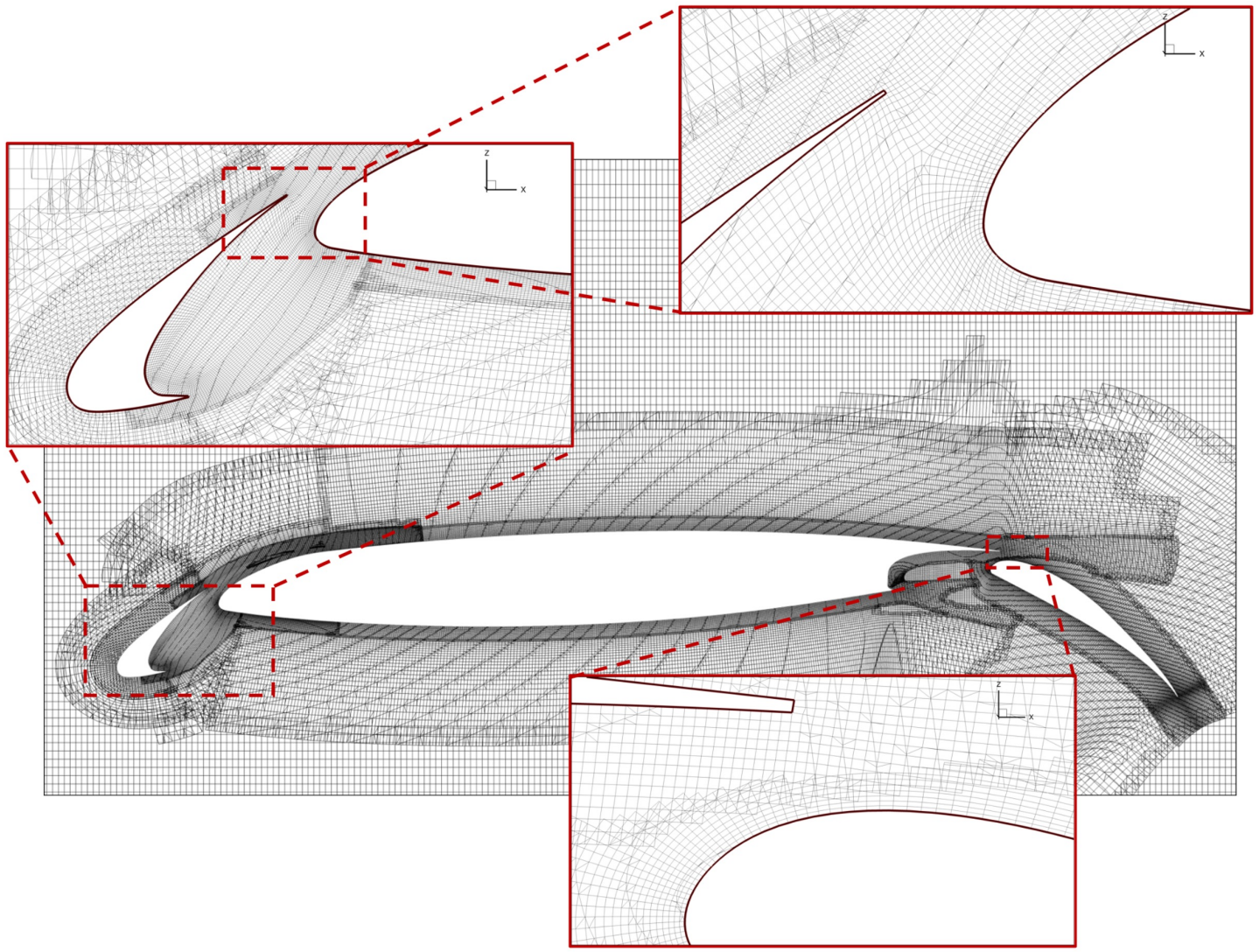
Grid Generation



RULES FOR CALCULATING WALL TIME:

1. Time-required after grid designed (spacings, aspect ratios, etc. determined)
2. 1 person for grid generation
3. Includes time for geometry modifications (when needed)
4. Assumes that a watertight CAD is available

Grid Generation

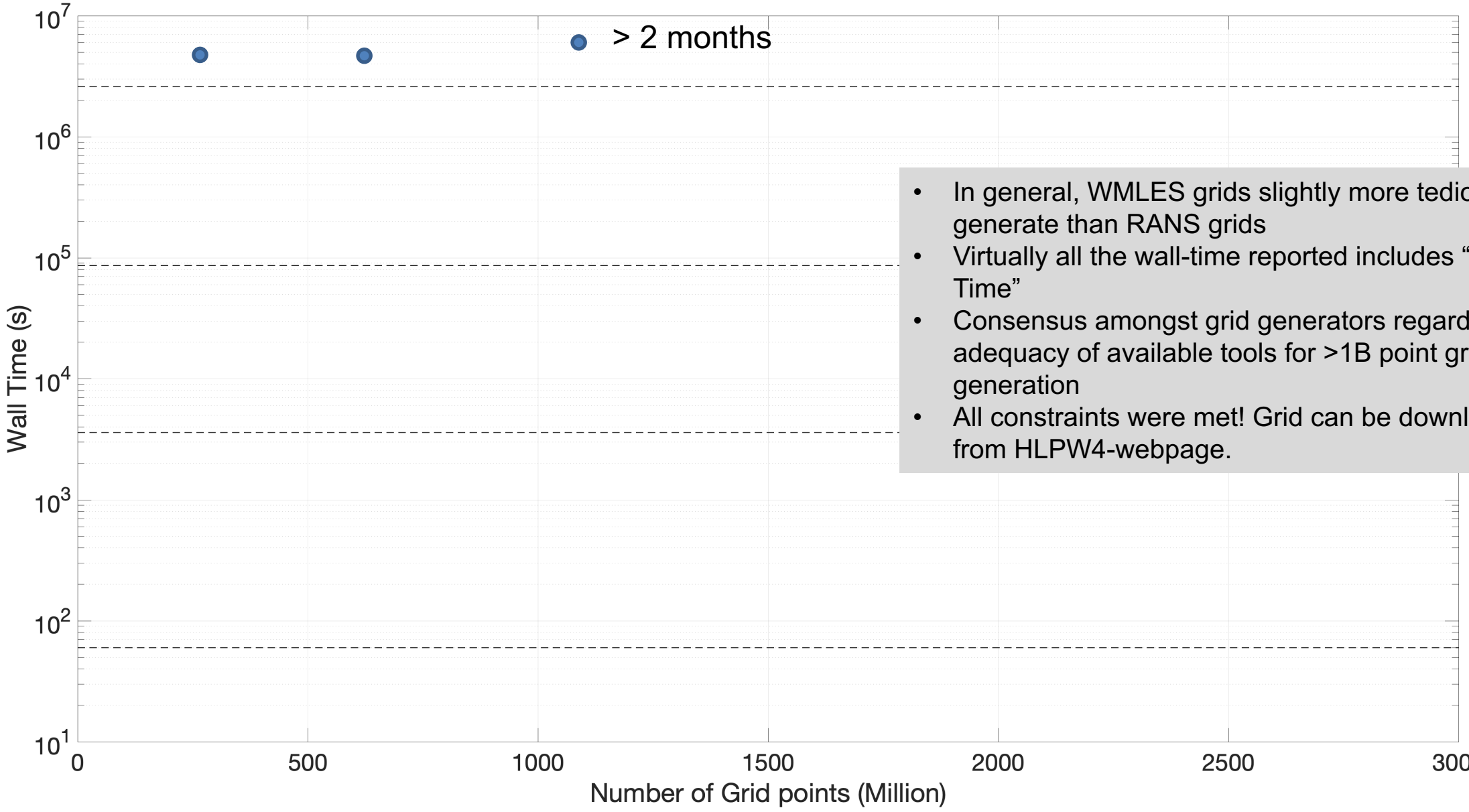


CURVILINEAR OVERSET GRIDS

- Grids generated by a **large group (8) of individuals** working on separate components
- WMLES-specific criteria for curvilinear grids:
  a. Minimum edge-length
  b. Cell-quality/skewness
  c. Max-aspect ratio
  d. Multiblock preferred over overset
  e. Corners need be represented as “sharp”
- For curvilinear grids, following folks were polled:
  A. Jared Duensing
  B. Luis dos Santos Fernandes
  C. Jeffrey Housman
  D. Gaetan Kenway
  E. Leonardo Machado
  F. Elisha Makarevich
  G. Daniel Maldonado
  H. Gerrit-Daniel Stich
- Utilized Pointwise + Chimera Grid Tools
- Some minor geometry modifications needed (See Seminar talk by Jared Duensing)

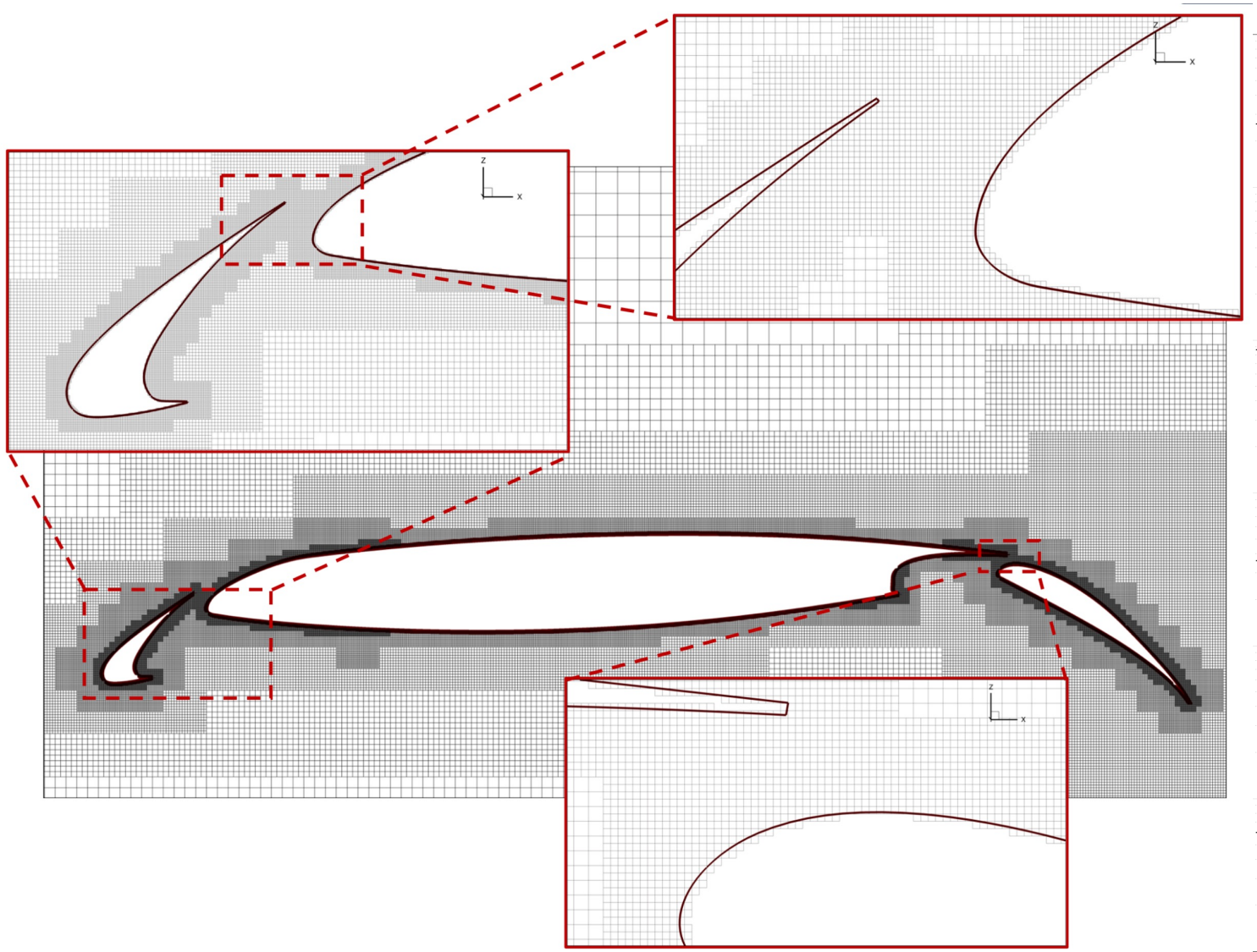


Grid Generation



- In general, WMLES grids slightly more tedious to generate than RANS grids
- Virtually all the wall-time reported includes “Human Time”
- Consensus amongst grid generators regarding in-adequacy of available tools for >1B point grid generation
- All constraints were met! Grid can be downloaded from HLPW4-webpage.

Grid Generation

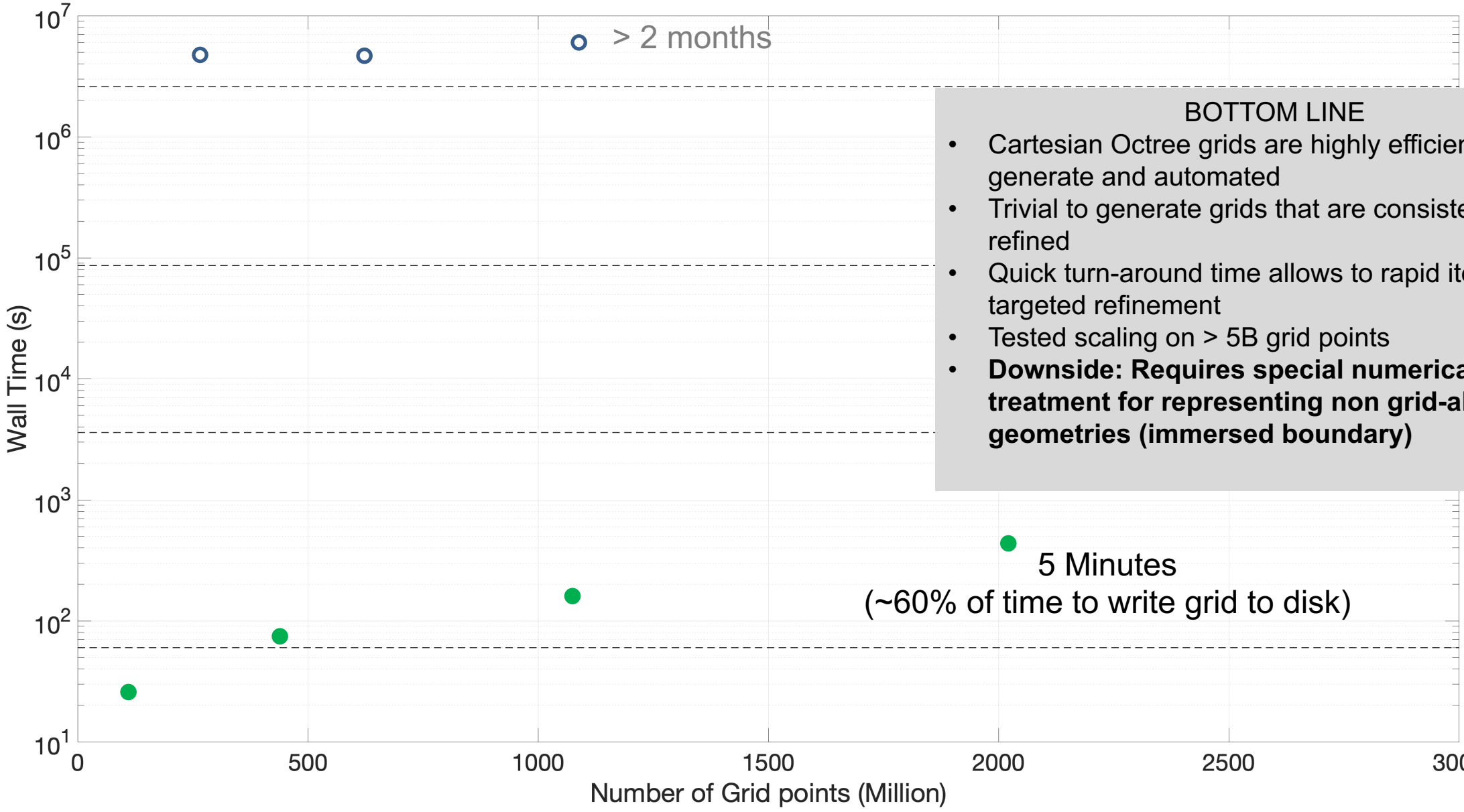


CARTESIAN OCTREE GRIDS

- Triangulation generated by Daniel Maldonado (Approx. 30mins using ANSA)
- No Geometry changes needed
- Octree grid generated using LAVA octree grid generator developed by Gaetan Kenway
- Small-box sizes for refinement reduces total node count
- All Constraints satisfied



Grid Generation



BOTTOM LINE

- Cartesian Octree grids are highly efficient to generate and automated
- Trivial to generate grids that are consistently refined
- Quick turn-around time allows to rapid iteration and targeted refinement
- Tested scaling on > 5B grid points
- **Downside: Requires special numerical treatment for representing non grid-aligned geometries (immersed boundary)**

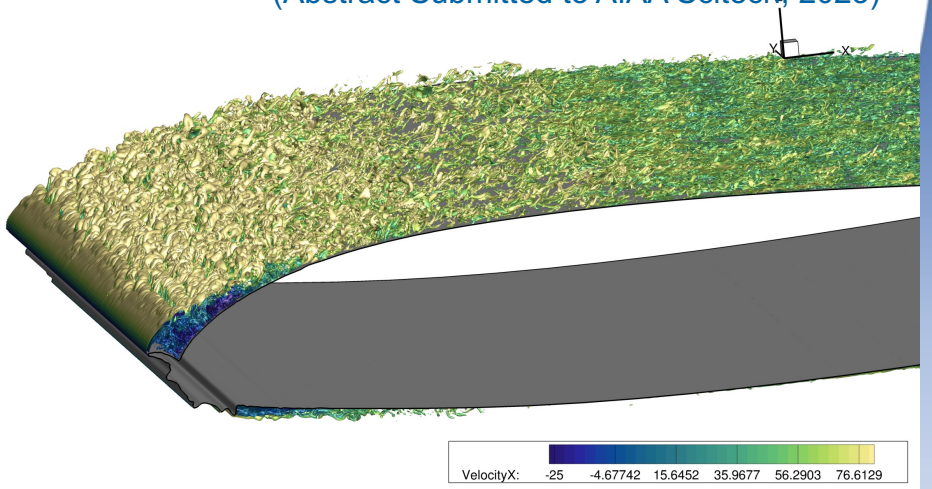
New Capability: Immersed Boundary WMLES in LAVA

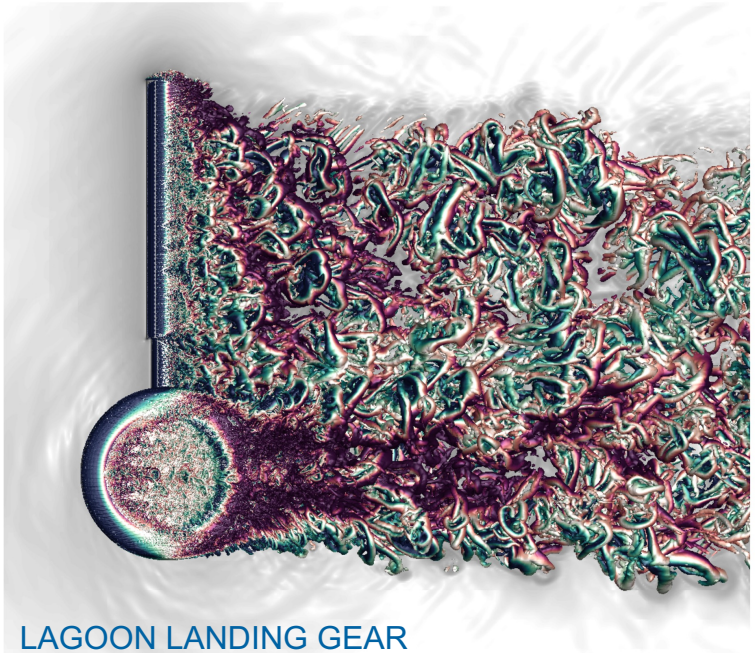
- Uses a **Ghost Cell Method** to impose inviscid boundary conditions at the wall
- **4th order accurate inviscid flux discretization** (order/stencil not changed near walls); 2nd order interpolation for image point probing
- New immersed boundary method developed (*journal manuscript under preparation*):
  - **Complex geometry handling:** Fully consistent ghost cells are used regardless of geometry complexity (sharp corners, thin edges) – required special data structures for ghost cells to take stencil-specific values).
  - **Spurious dilatational and entropic content** : Numerical treatment to address spurious modes without filtering or upwinding near smooth-walls (very relevant for coarse-grid WMLES)
  - **Wall-Stress treatment:** The formulation ensures that the full-wall stress is applied when boundary stress-tensors are rotated in the wall-aligned frame of reference and momentum conservation in this rotated frame is enforced at the walls.
- Stencil based upwinding **only applicable at trapped-cells**: use 3rd order WENO (Jiang & Shu, 2002) interpolation locally

New Capability: Immersed Boundary WMLES in LAVA

- Canonical problems studied show similar resolution requirements (points per δ) compared to curvilinear:
  a. Flat plate BL at $0°$ (geometry aligned with grid) and $23°$ (maximum mass-flux error due to mis-alignment)
  b. NASA Wall-Mounted Hump: Velocity/Stress Profiles, cp and cf
  c. LAGOON Landing Gear: Noise Prediction
  d. Iced (EG1164) NACA 23012: Aerodynamic Load predictions (separated flows)
  e. Axisymmetric Transonic Cold Jet (near-field validation)
  f. Gaussian Bump (Ongoing)
  g. Buffet applications (Ongoing) - Two Scitech 2023 abstracts submitted

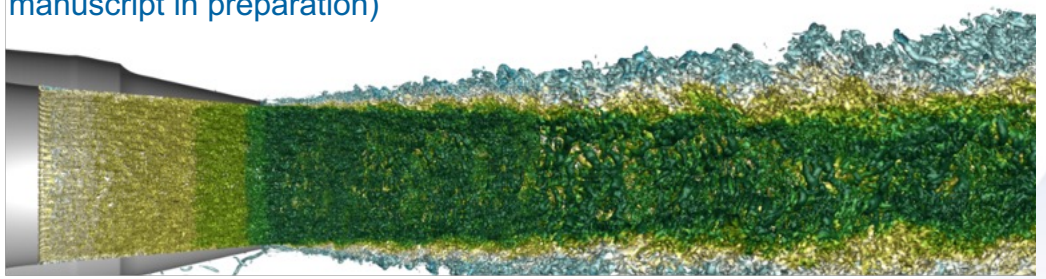
NACA 23012 + EG 1165 ICING
(Abstract Submitted to AIAA Scitech, 2023)



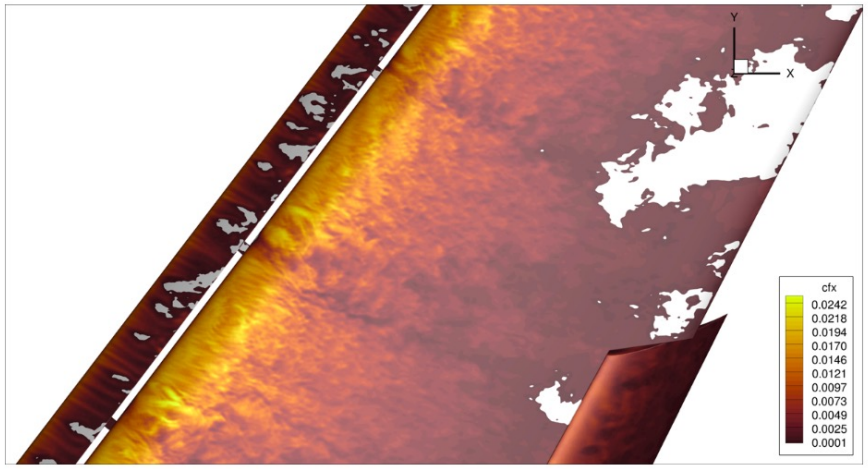


LAGOON LANDING GEAR
(See Wong et al., AIAA Aeroacoustics Conference, 2022)

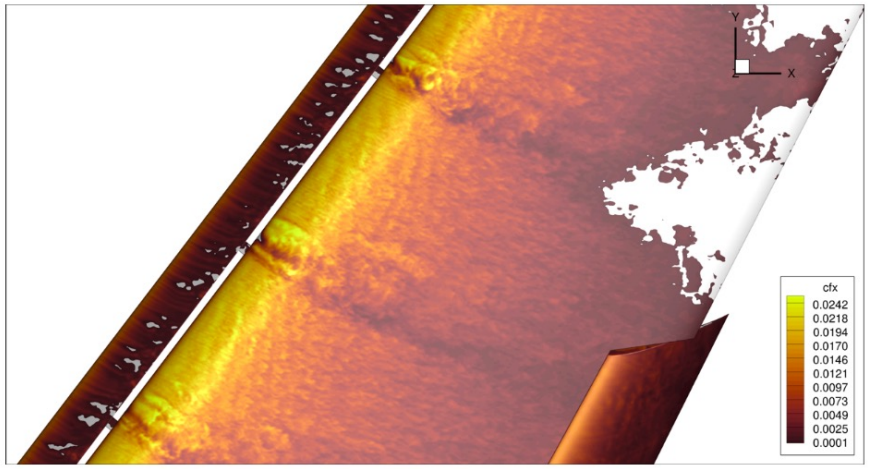
AXISYMMETRIC TRANSONIC COLD JET
(Journal manuscript in preparation)



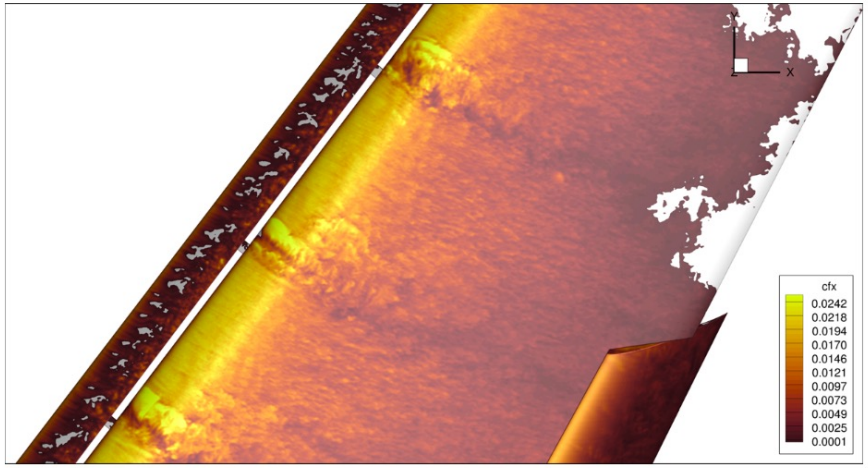
New Capability: Immersed Boundary WMLES in LAVA



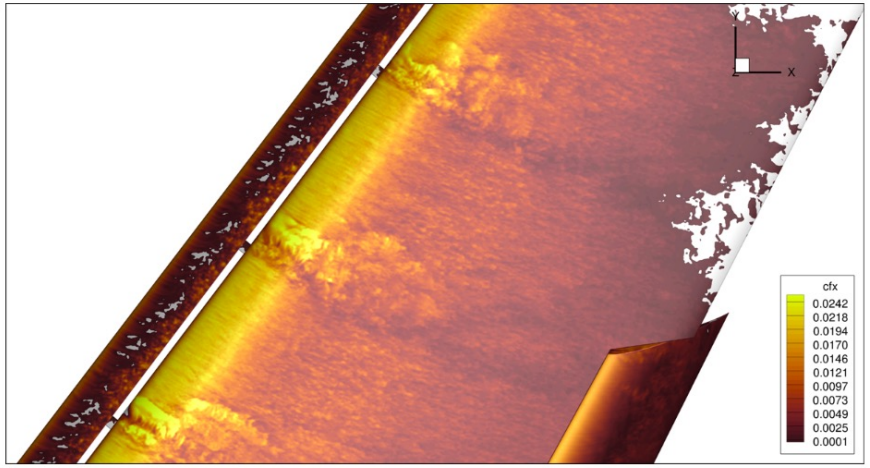
(a) 12mm Grid (100M)



(b) 6mm Grid (450M)



(c) 4mm Grid (1100M)



(d) 3mm Grid (2020M)

Midboard/Outboard wing at CLmax,
Instantaneous c_{Fx}
Blanked Regions depict $c_{Fx} < 0$

Special emphasis on:

- Avoiding spurious stair-stepping or Cartesian Imprinting
- Numerically transitioned BLs should not have Cartesian-effects
- No tunable artificial “tripping” – flow transitions on its own

Discretization for LAVA WMLES

Curvilinear vs. Cartesian Discretizations

Similarities:

- Constant coefficient Vreman model (little sensitivity observed to model constant at CLmax)
- 2nd order staggered viscous flux discretization
- Localized upwinding (3rd order linear upwind biased interpolation) based on a Ducros-Type sensor
- Explicit Time-stepping using 3rd order RK (similar CFL values)

Differences:

- Curvilinear uses 2nd order derivative of flux; Cartesian uses 4th order derivative of flux (Nonomura et al., 2013)
- Curvilinear uses wall-function by Musker (1979); Cartesian uses a custom blended function (lower cost)
- Curvilinear uses WM exchange at $2\Delta_x$; Cartesian uses WM exchange at $1\Delta_x$ from wall (little sensitivity reported at CLmax)
- When upwinding is active, Curvilinear uses HLL Riemann Solver, Cartesian uses HLLC Riemann Solver (little sensitivity; mostly cost considerations)

Grid Summary

SUMMARY OF GRID SYSTEMS STUDIED

Name	Solve Points	Off-wall spacing	Nominal Aspect Ratio	Comments
Grid W-A	275M	5mm (2.5mm near LE and flaps)	6-8	Baseline Curvilinear Grid
Grid W-B	360M	5mm (2.5mm near LE and flaps)	6-8	Grid W-A + (a)
Grid W-C	650M	5mm (2.5mm near LE and flaps)	2-3	Grid W-B + (b)
Grid W-D	1100M	2.5mm (5mm on wing pressure side)	4-6	Grid W-C + (c)
12mm, 100M	**100M**	**12mm (Isotropic)**	**1**	**Baseline Cartesian Octree Grid**
6mm, 450M	**450M**	**6mm (Isotropic)**	**1**	**Global Refinement**
4mm, 1100M	**1100M**	**4mm (Isotropic)**	**1**	**Global Refinement**
3mm, 2020M	**2020M**	**3mm (Isotropic)**	**1**	**Global Refinement**
3mm/6mm, 1000M	**1000M**	**3mm + 6mm (Isotropic)**	**1**	**Targeted Refinement**

← Deemed "Best-practice"; used for in-tunnel simulations

← Deemed "Best-practice"

Curvilinear Grid Refinement:

(a): Off-body refinement (plus new block for chine-vortex)

(b): Surface grid refinement (aspect ratios close to unity)

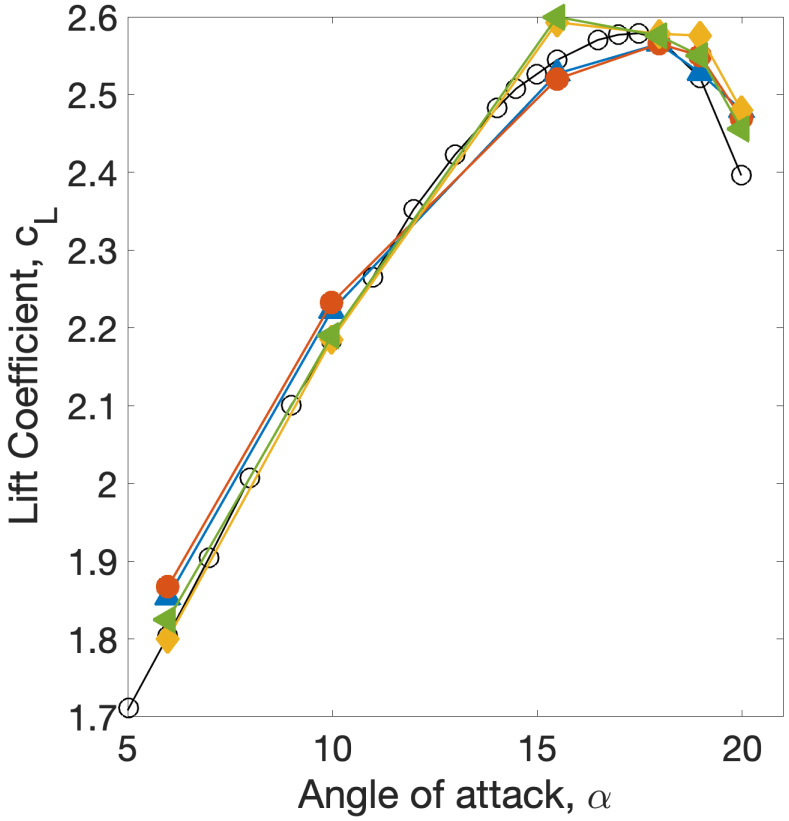
(c): Wall-normal refinement (2x refinement on suction surfaces)

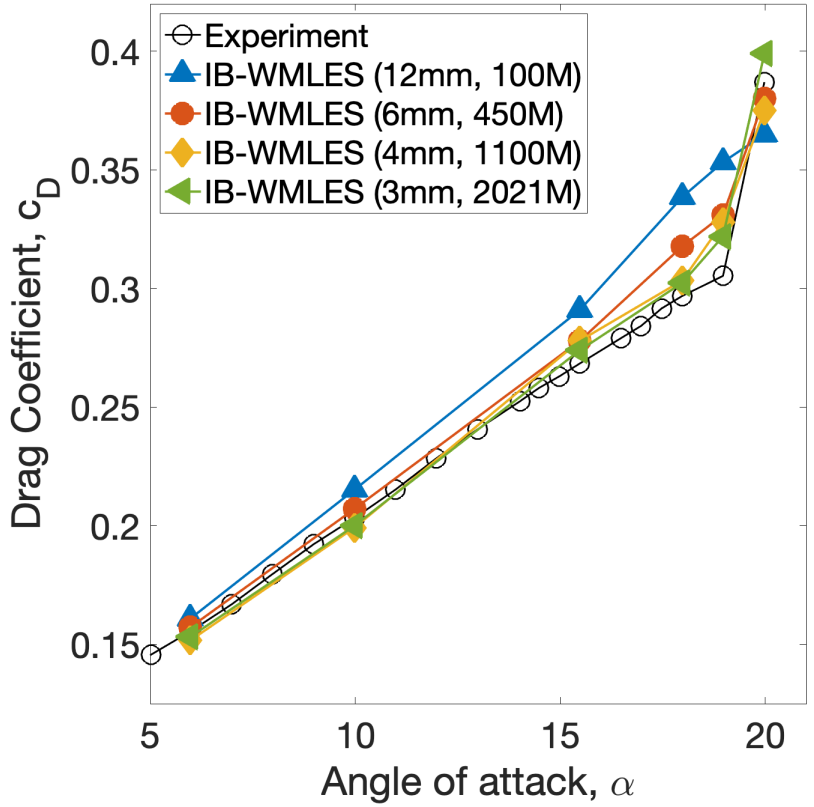
Cartesian Octree Targeted Refinement:

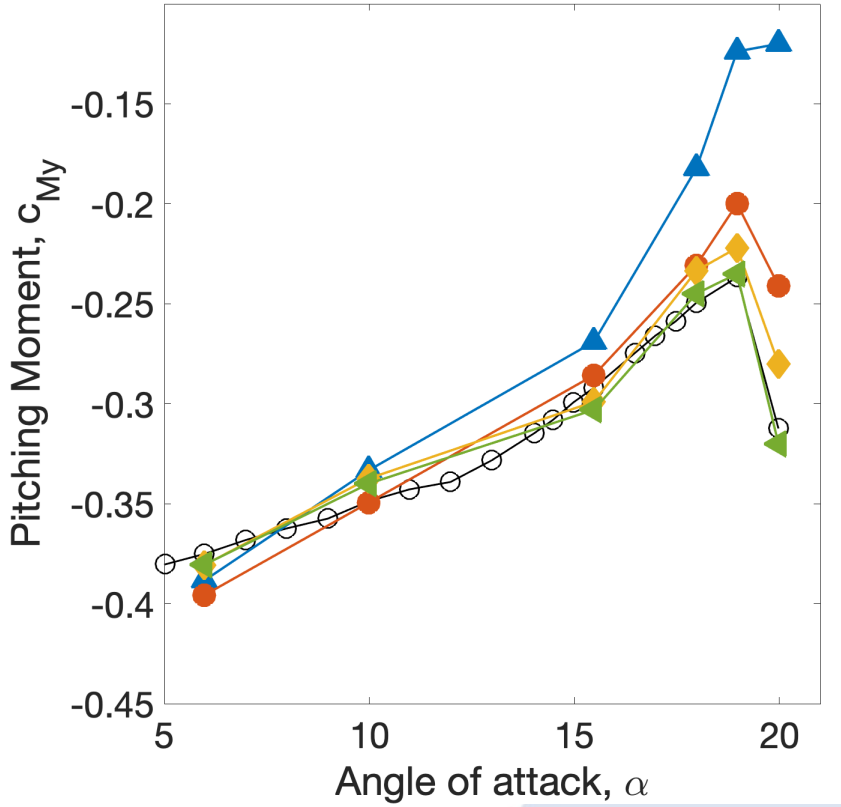
(Discussed later)

Part A: In-Tunnel WMLES

In-Tunnel Simulations







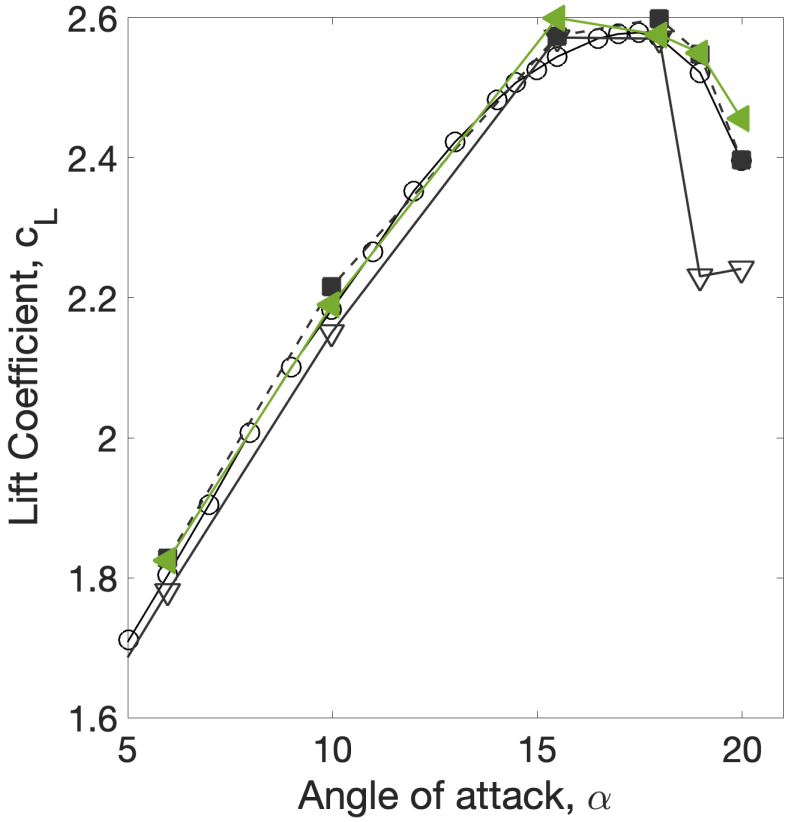
Refer to paper for information on:

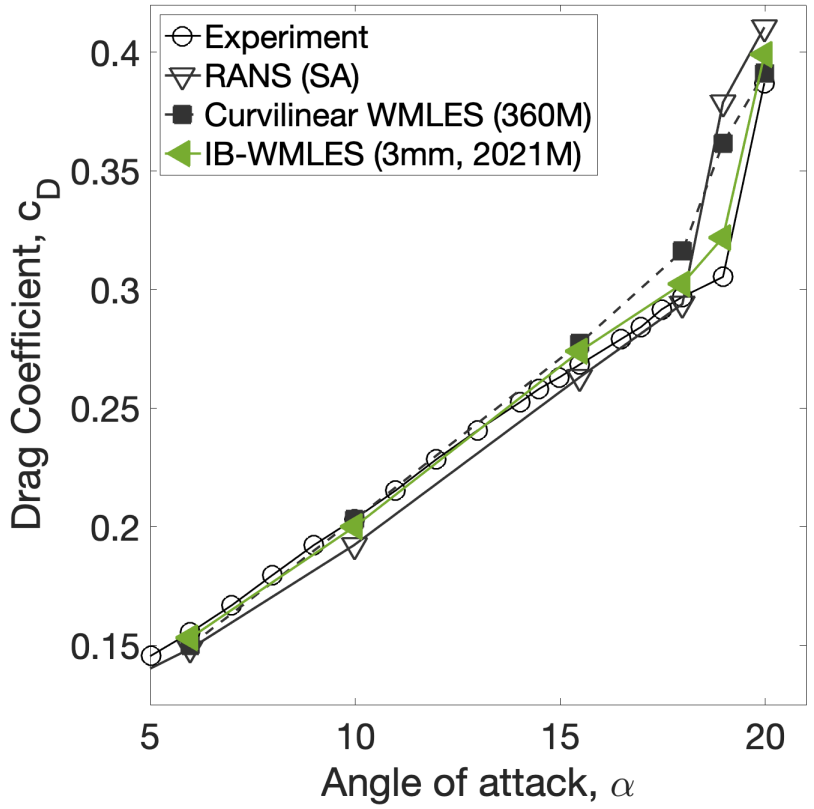
1. Initialization procedure (tunnel back-pressure)
2. Tunnel floor BL comparisons with rake data

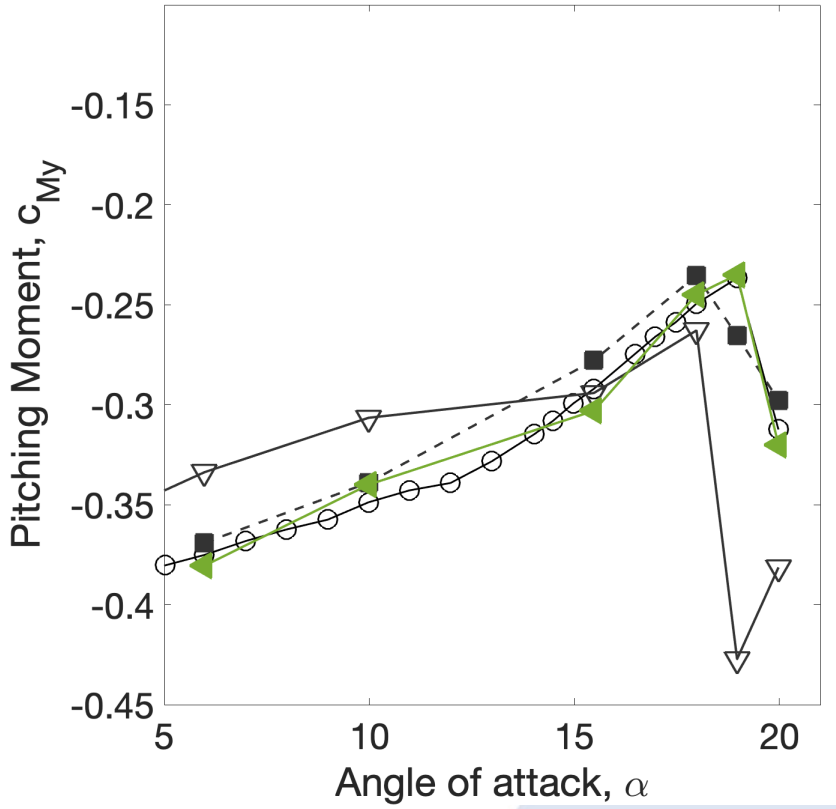
After interpolation to primary/final grid:

1. Transience washout: 10-20 CTU
2. Statistical averaging: 10-30 CTU ($\alpha < 18^\circ$) and 80 CTU ($\alpha > 18^\circ$)

In-Tunnel Simulations







Refer to paper for information on:

1. Initialization procedure (tunnel back-pressure)
2. Tunnel floor BL comparisons with rake data

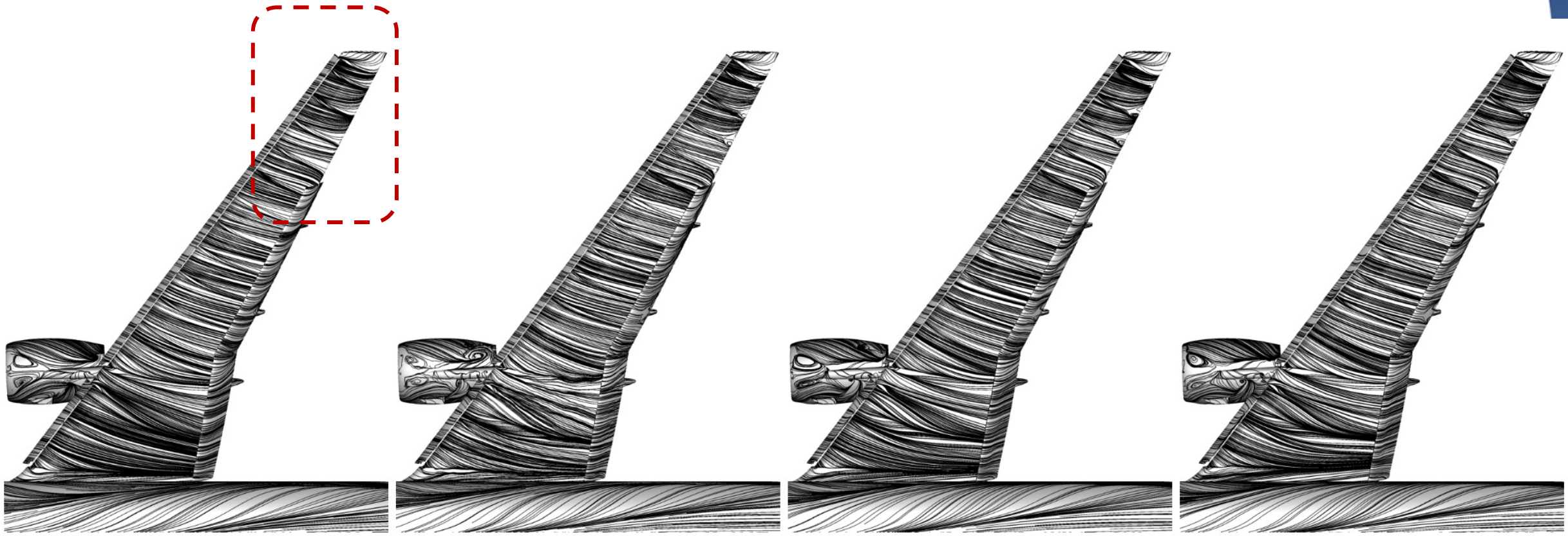
After interpolation to primary/final grid:

1. Transience washout: 10-20 CTU
2. Statistical averaging: 10-30 CTU ($\alpha < 18^\circ$) and 80 CTU ($\alpha > 18^\circ$)

In-Tunnel Simulations – Cartesian IB-WMLES

$$\alpha = 15.48^{\circ}$$

Time-averaged surface streamlines

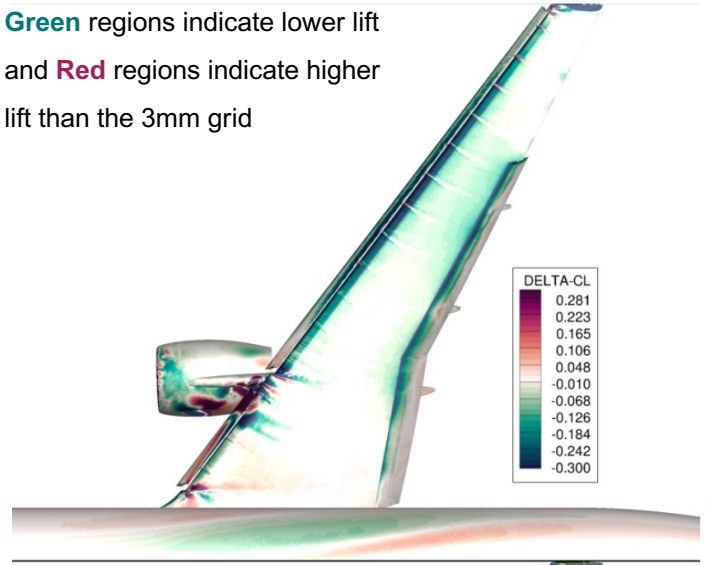


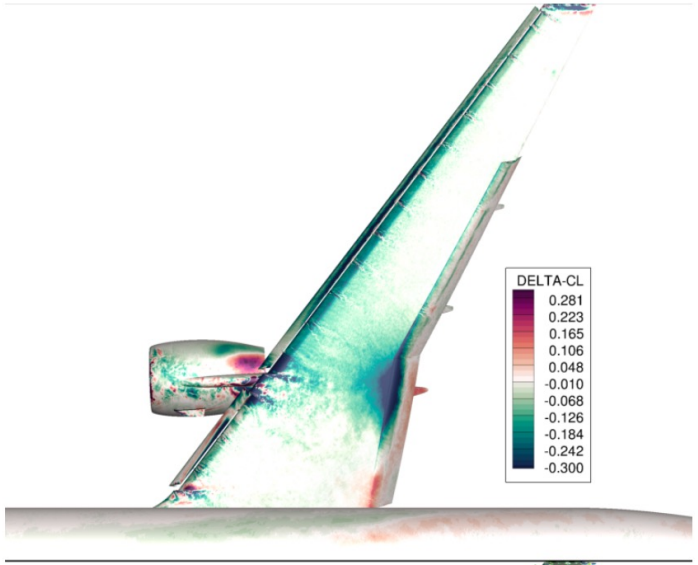
(a) 12mm Grid (100M) (b) 6mm Grid (450M) (c) 4mm Grid (1100M) (d) 3mm Grid (2021M)

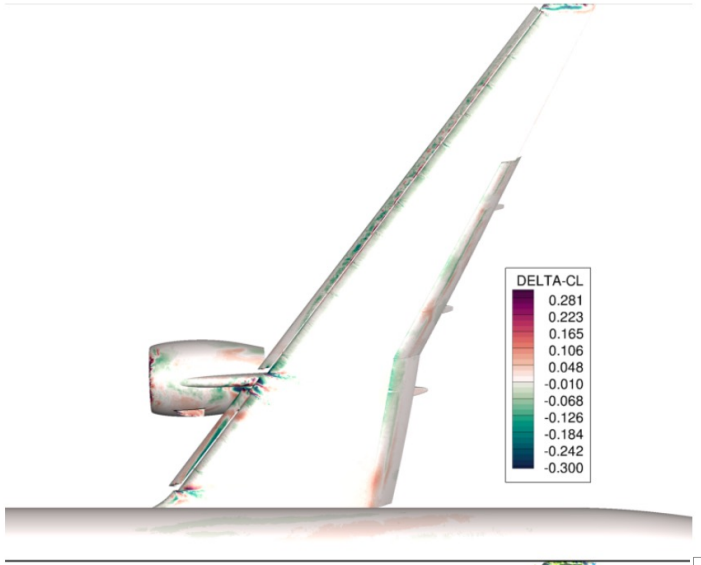
In-Tunnel Simulations – Cartesian IB-WMLES

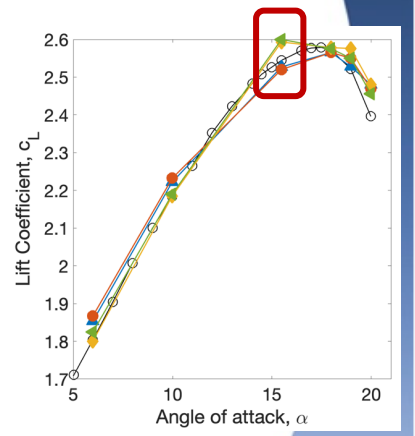
$\alpha = 15.48^{\circ}$

Green regions indicate lower lift and **Red** regions indicate higher lift than the 3mm grid

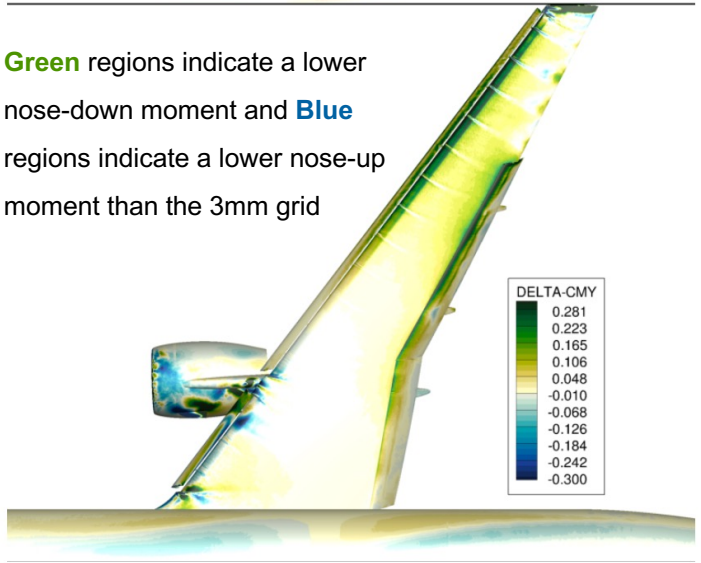


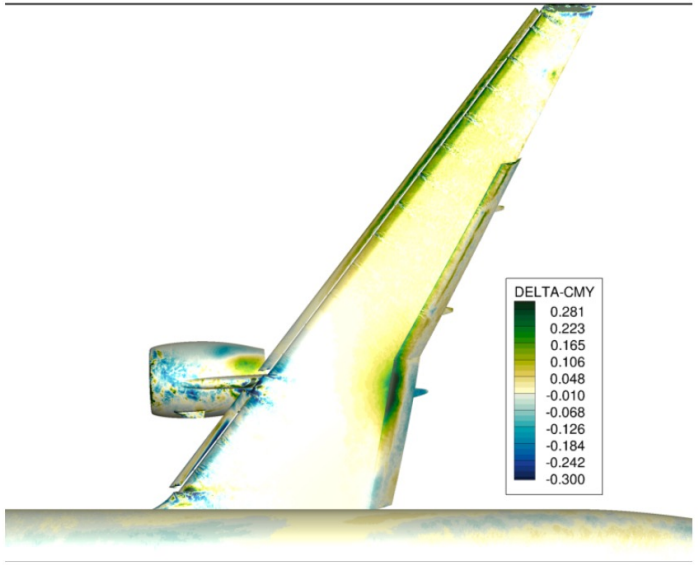


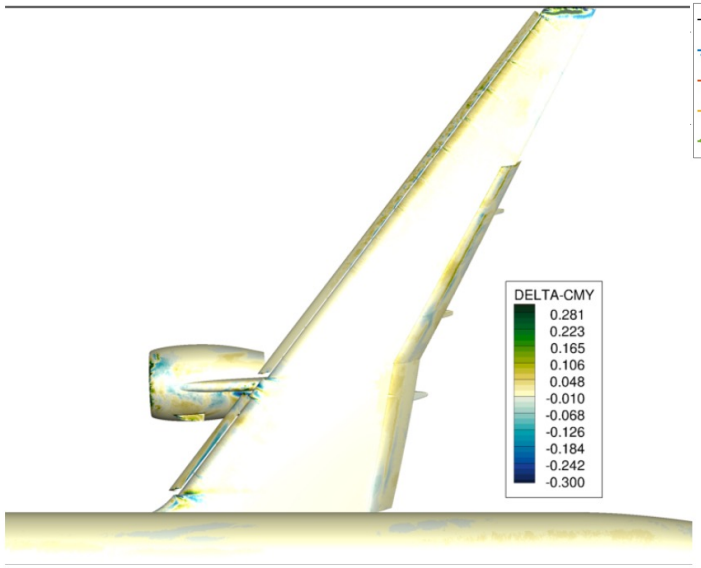




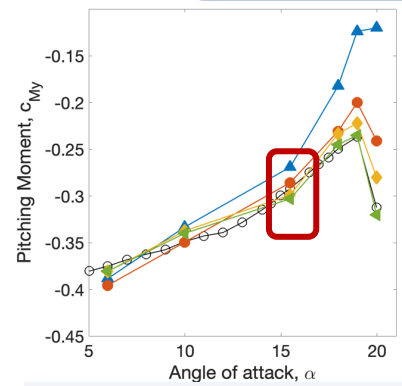
Green regions indicate a lower nose-down moment and **Blue** regions indicate a lower nose-up moment than the 3mm grid











(a) 12mm Grid (100M)

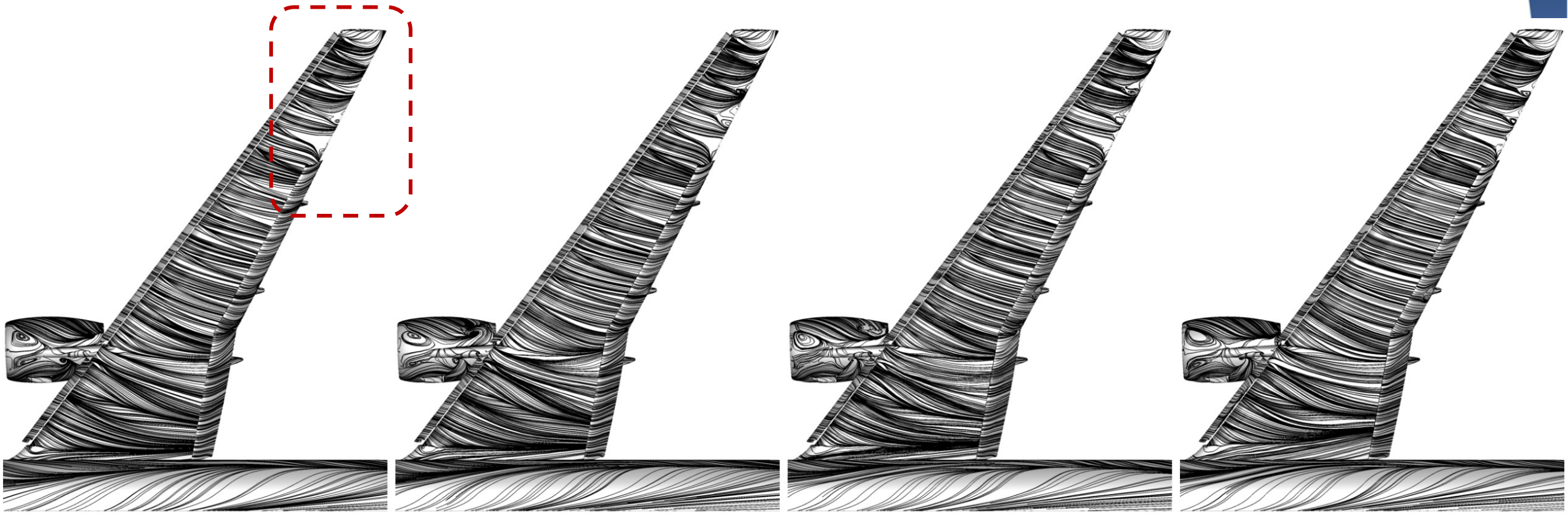
(b) 6mm Grid (450M)

(c) 4mm Grid (1100M)

In-Tunnel Simulations – Cartesian IB-WMLES

$$\alpha = 17.98^{\circ}$$

Time-averaged surface streamlines



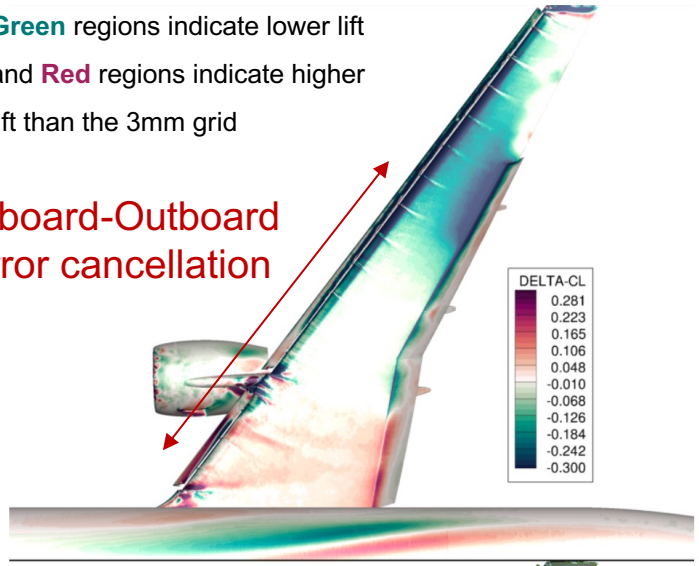
(a) 12mm Grid (100M) (b) 6mm Grid (450M) (c) 4mm Grid (1100M) (d) 3mm Grid (2021M)

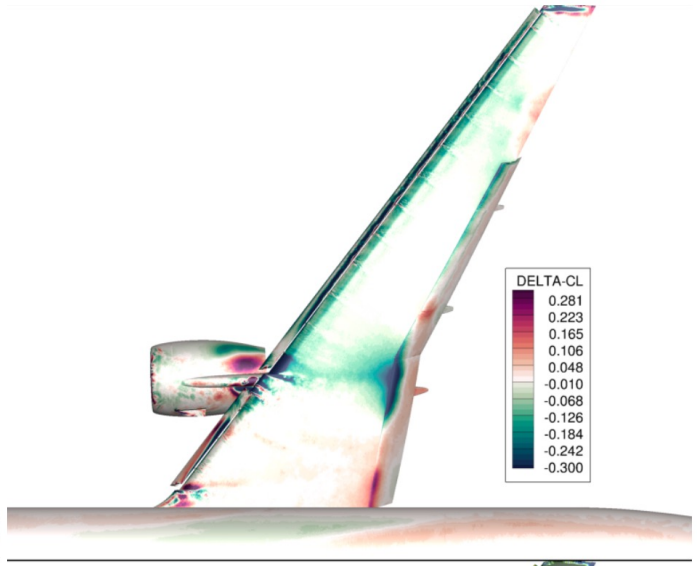
In-Tunnel Simulations – Cartesian IB-WMLES

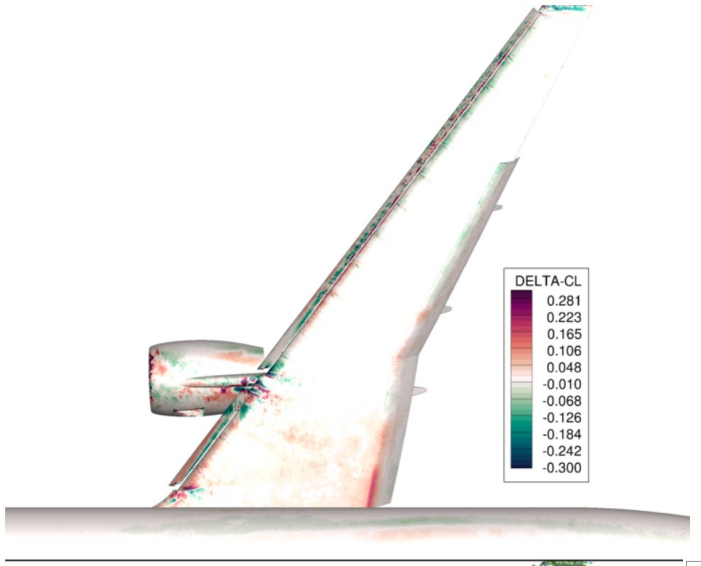
$\alpha = 17.98°$

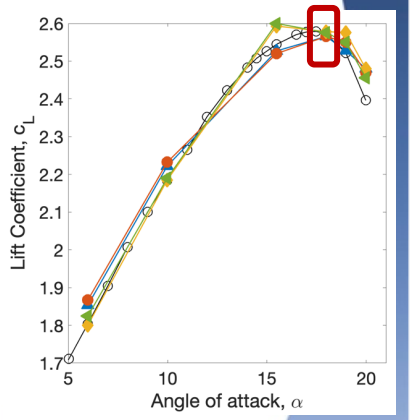
Green regions indicate lower lift and **Red** regions indicate higher lift than the 3mm grid

Inboard-Outboard error cancellation



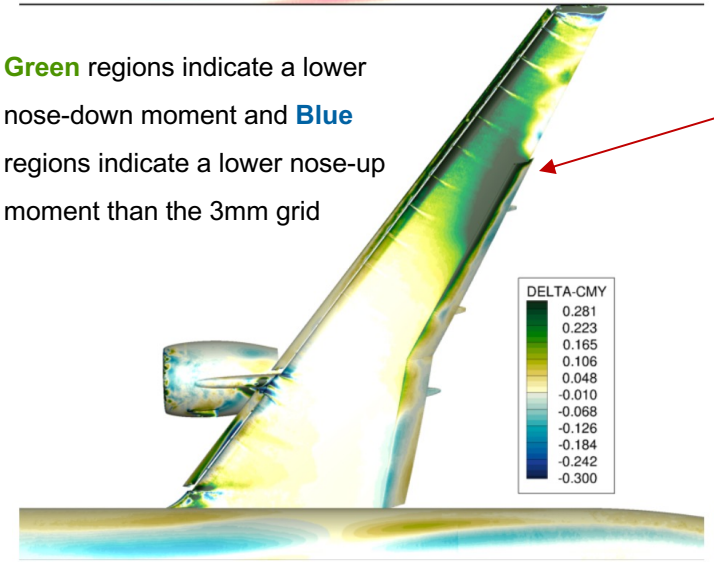


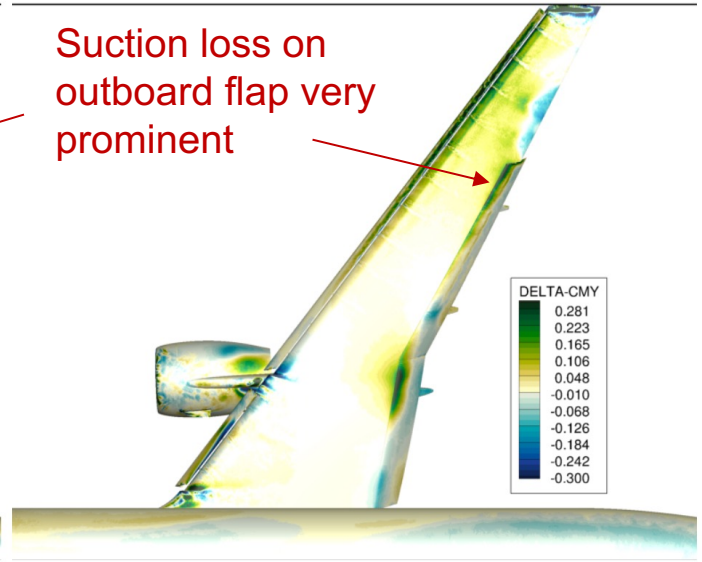


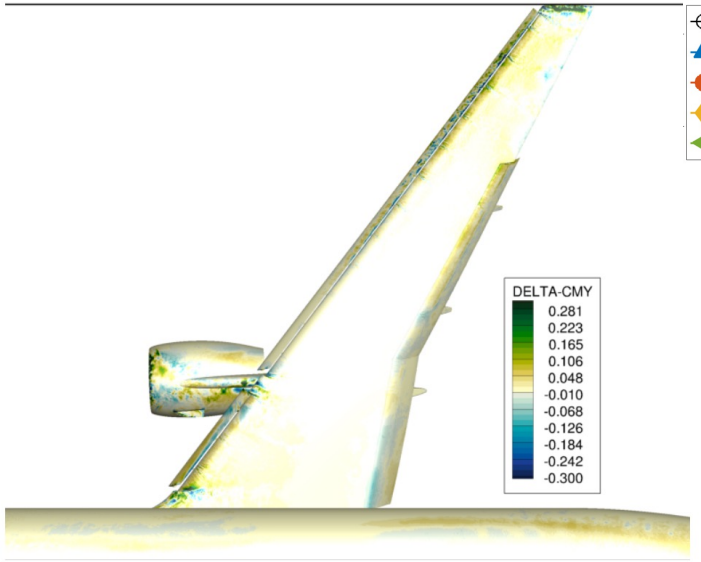


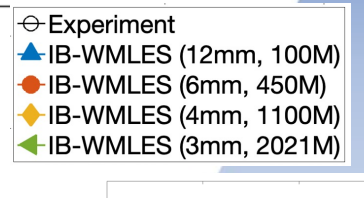
Green regions indicate a lower nose-down moment and **Blue** regions indicate a lower nose-up moment than the 3mm grid

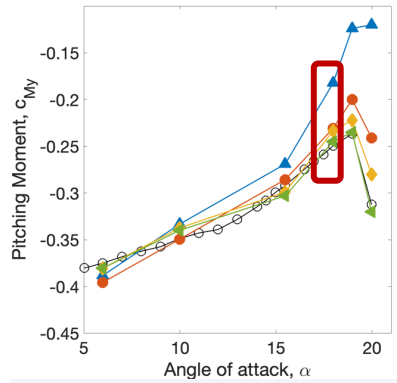
Suction loss on outboard flap very prominent









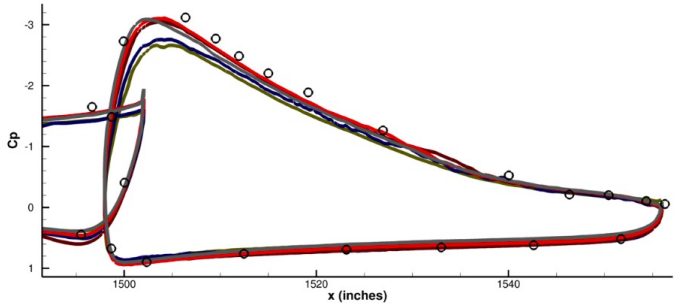


(a) 12mm Grid (100M)

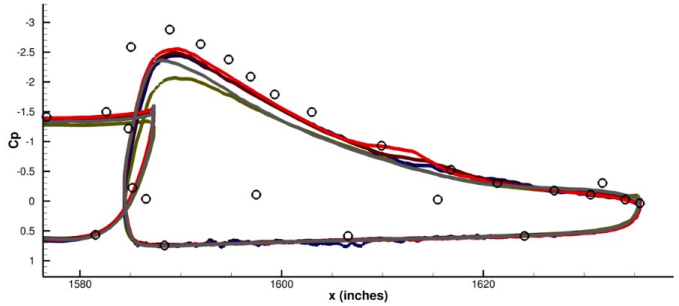
(b) 6mm Grid (450M)

(c) 4mm Grid (1100M)

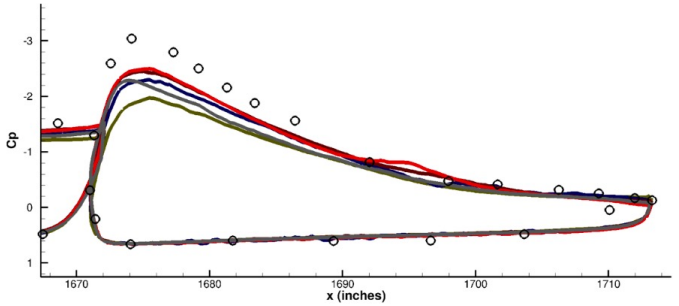
In-Tunnel Simulations



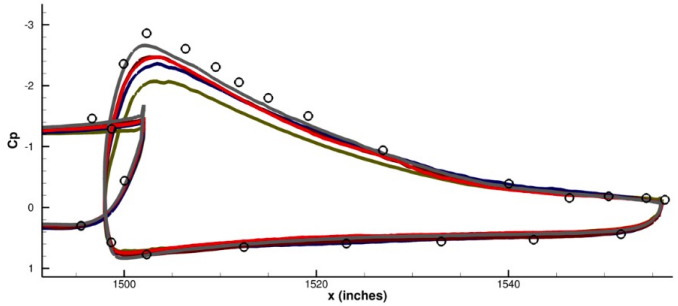
(a) $\alpha = 15.48°$, Section D, $\eta = 0.42$



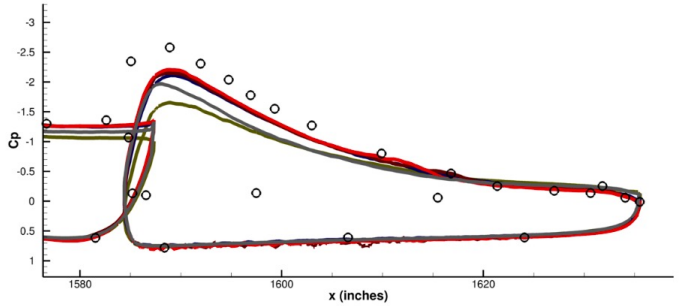
(b) $\alpha = 15.48°$, Section E, $\eta = 0.55$



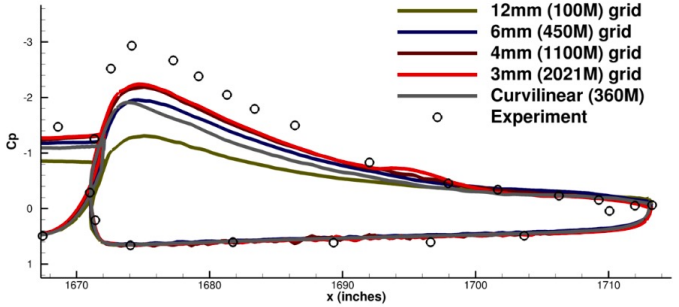
(c) $\alpha = 15.48°$, Section F, $\eta = 0.69$



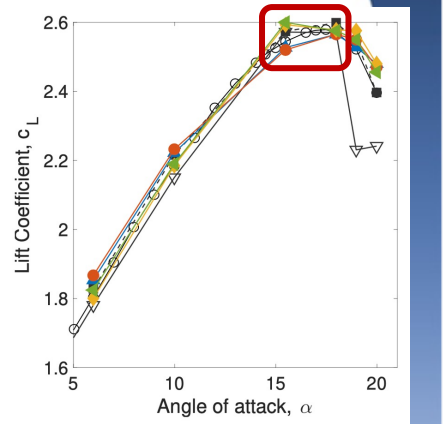
(d) $\alpha = 17.98°$, Section D, $\eta = 0.42$

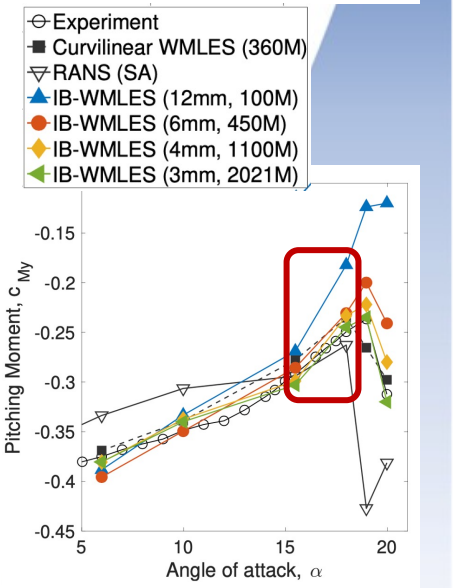


(e) $\alpha = 17.98°$, Section E, $\eta = 0.55$



(f) $\alpha = 17.98°$, Section F, $\eta = 0.69$



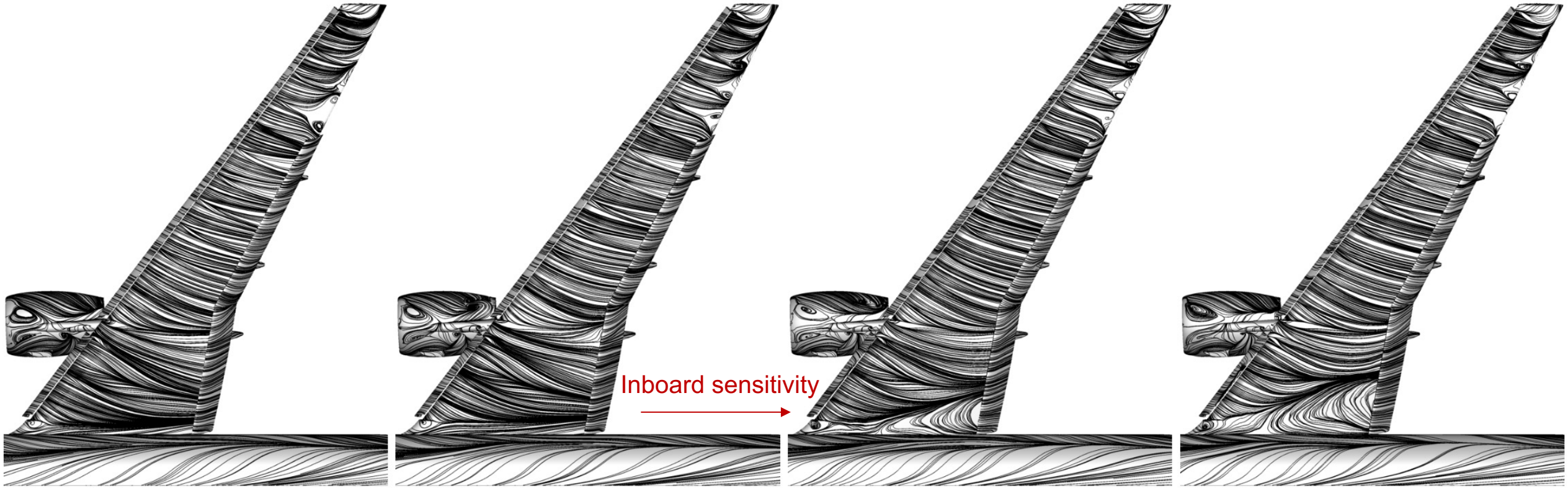


- Near CLmax, cartesian grids (3mm and 4mm) appear to be more accurate than curvilinear grid
- Little to no-variation between the 3mm and 4mm grids
- Section F flap suction peaks continue to be underpredicted by all simulations – does not go away with resolution increase

In-Tunnel Simulations – Cartesian IB-WMLES

$$\alpha = 18.97^{\circ}$$

Time-averaged surface streamlines



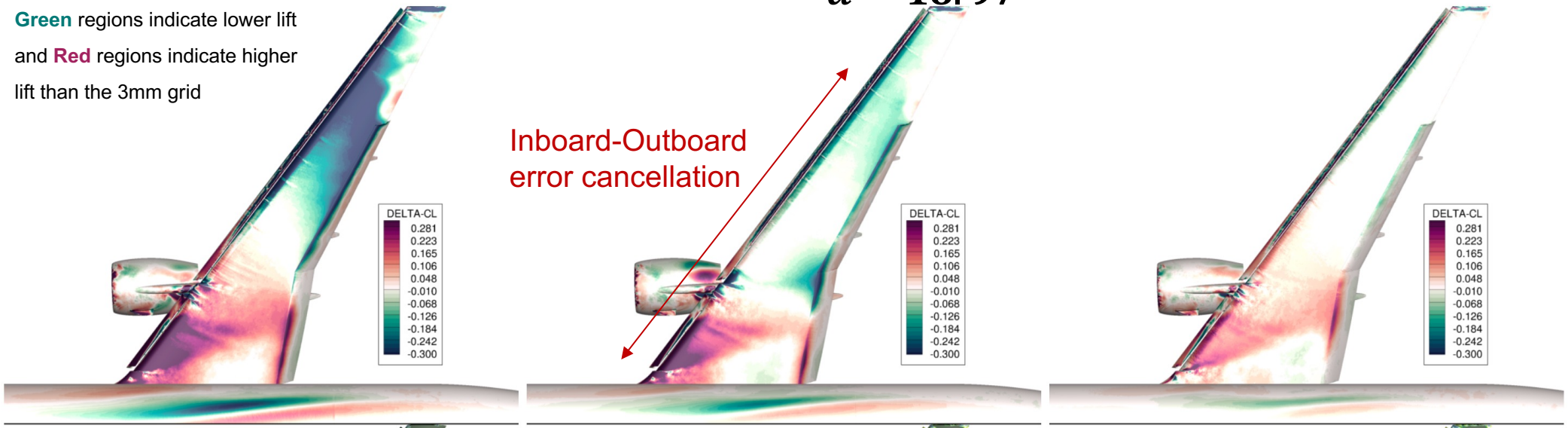
(a) 12mm Grid (100M) (b) 6mm Grid (450M) (c) 4mm Grid (1100M) (d) 3mm Grid (2021M)

In-Tunnel Simulations – Cartesian IB-WMLES

$\alpha = 18.97°$

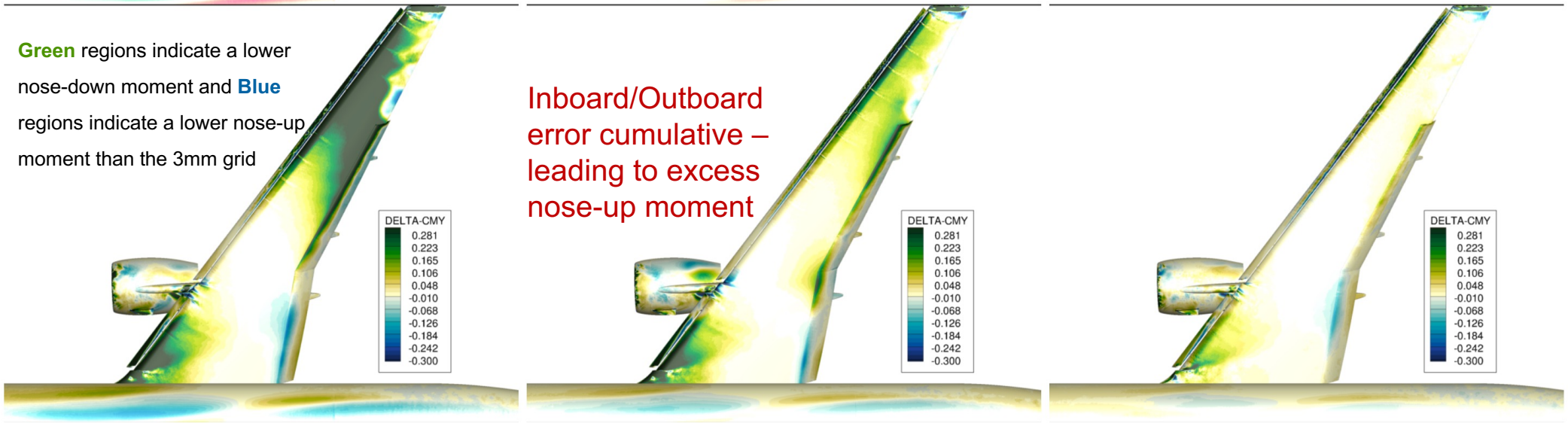
Green regions indicate lower lift and **Red** regions indicate higher lift than the 3mm grid

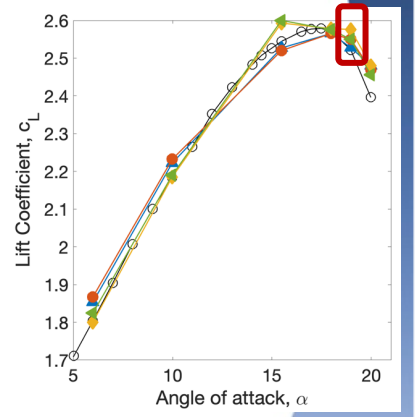
Inboard-Outboard error cancellation



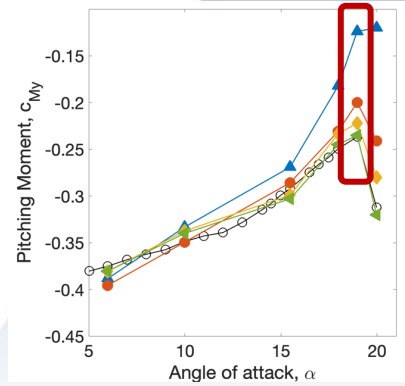
Green regions indicate a lower nose-down moment and **Blue** regions indicate a lower nose-up moment than the 3mm grid

Inboard/Outboard error cumulative – leading to excess nose-up moment









(a) 12mm Grid (100M)

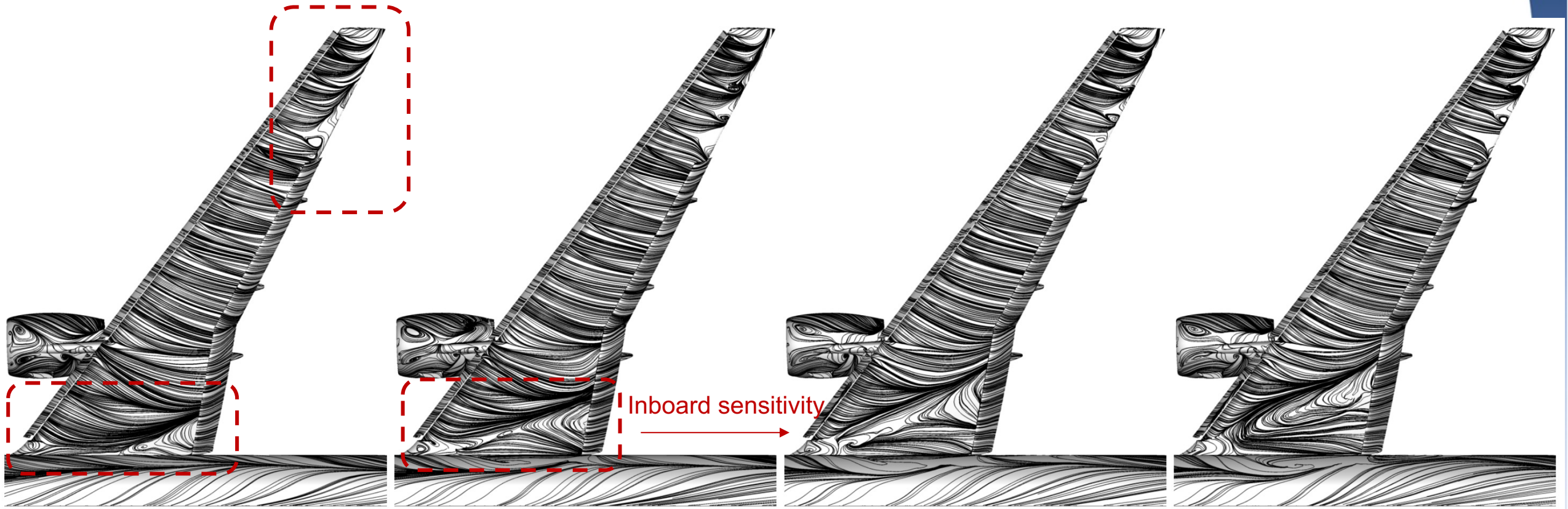
(b) 6mm Grid (450M)

(c) 4mm Grid (1100M)

In-Tunnel Simulations – Cartesian IB-WMLES

$$\alpha = 19.98^{\circ}$$

Time-averaged surface streamlines

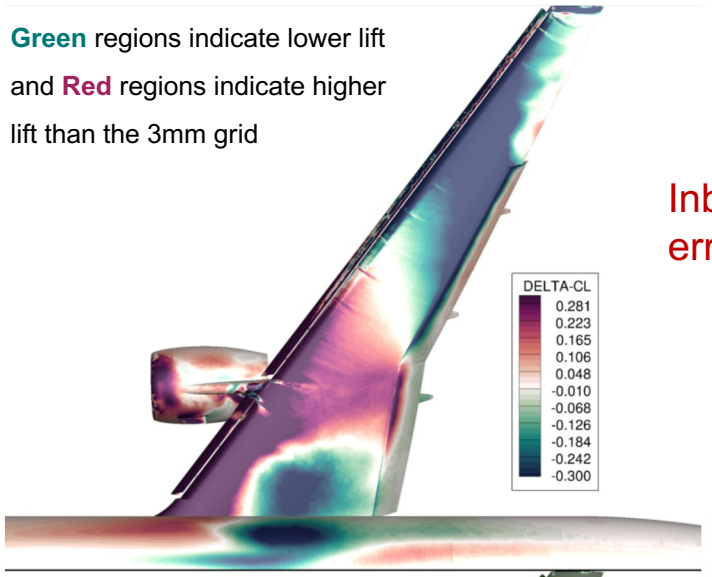


(a) 12mm Grid (100M) (b) 6mm Grid (450M) (c) 4mm Grid (1100M) (d) 3mm Grid (2021M)

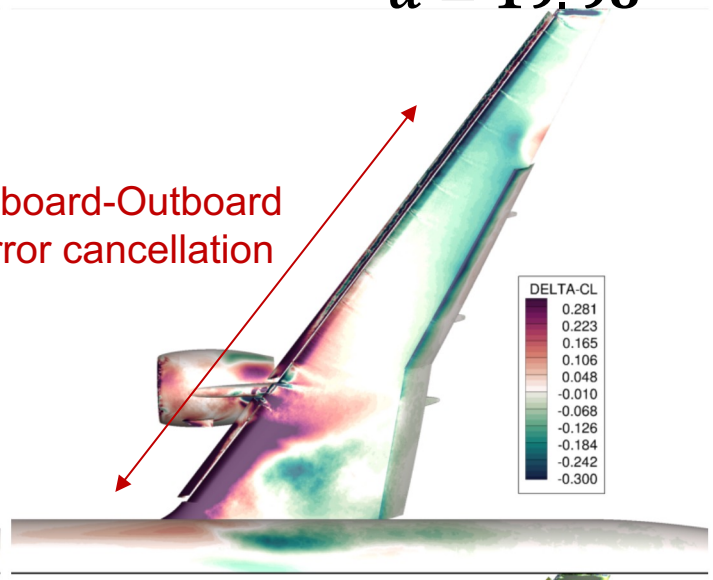
In-Tunnel Simulations – Cartesian IB-WMLES

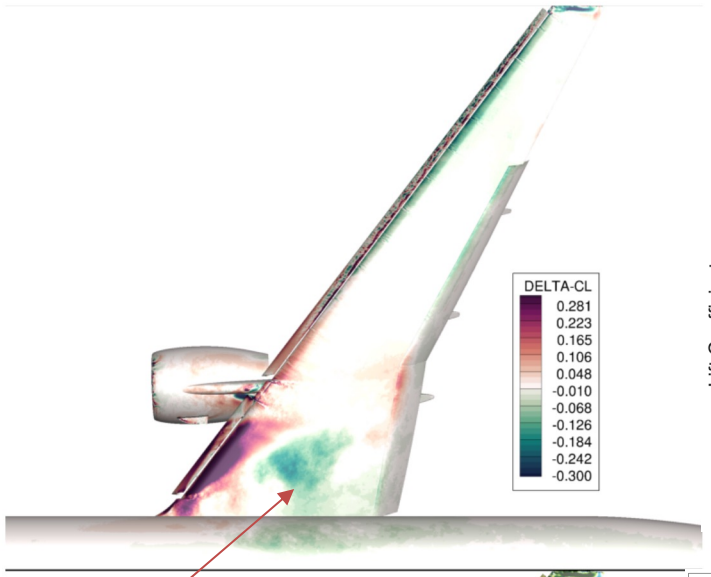
$\alpha = 19.98°$

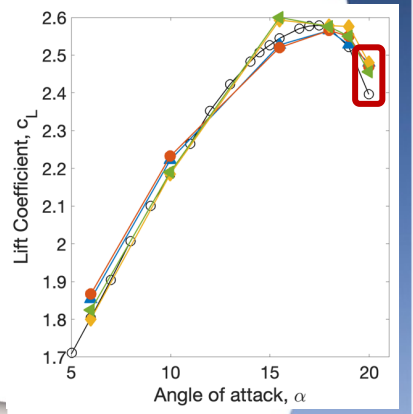
Green regions indicate lower lift and **Red** regions indicate higher lift than the 3mm grid



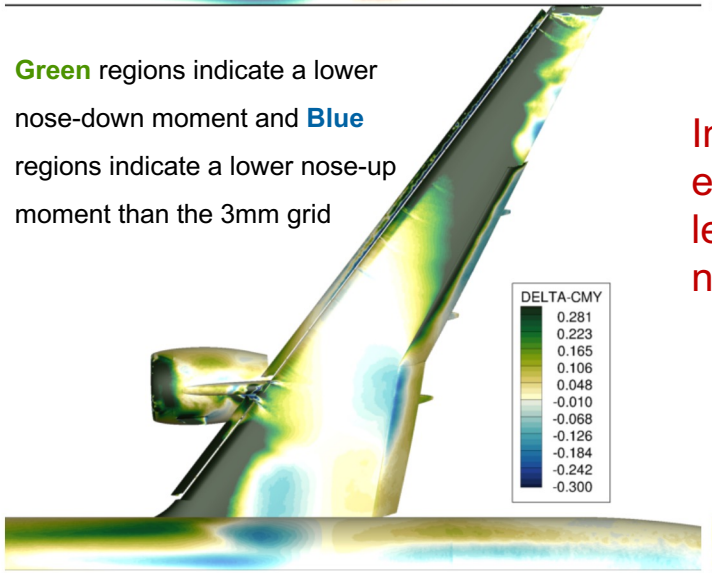
Inboard-Outboard error cancellation



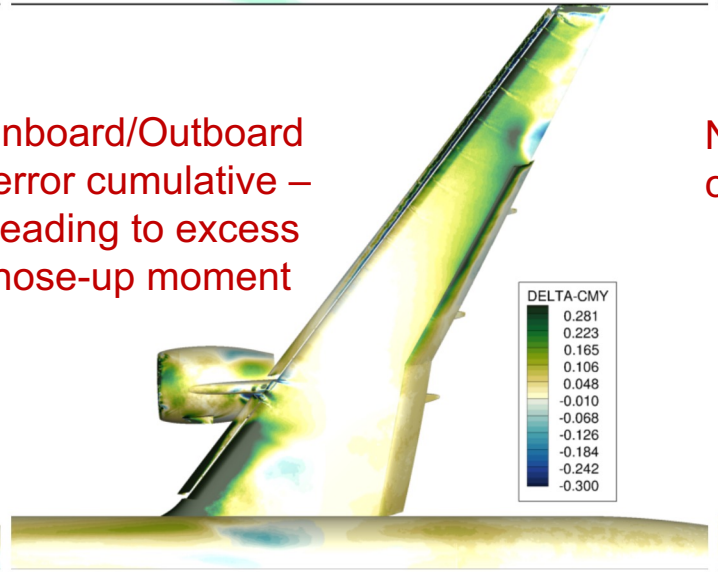




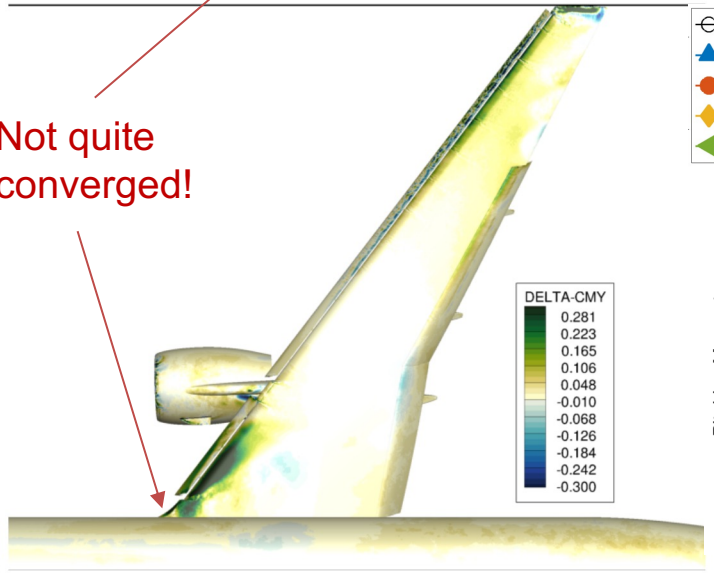
Green regions indicate a lower nose-down moment and **Blue** regions indicate a lower nose-up moment than the 3mm grid

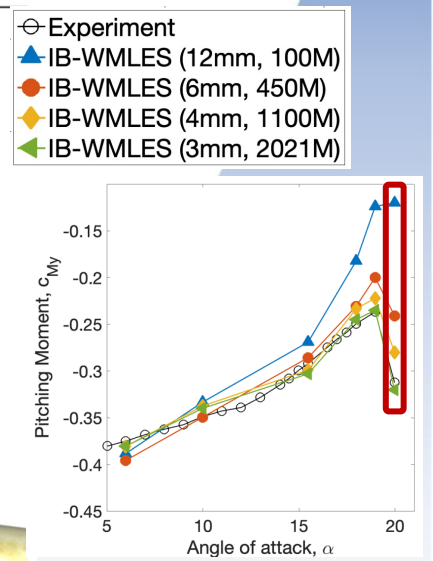


Inboard/Outboard error cumulative – leading to excess nose-up moment



Not quite converged!





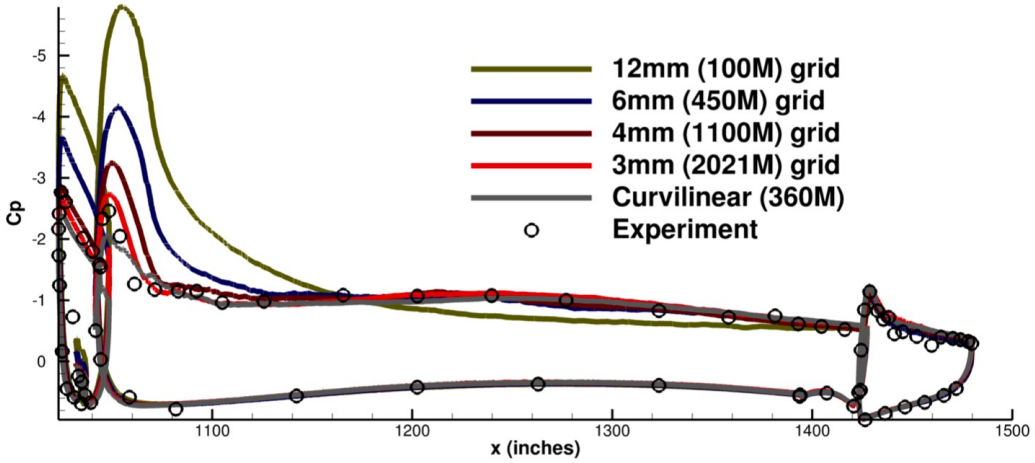
(a) 12mm Grid (100M)

(b) 6mm Grid (450M)

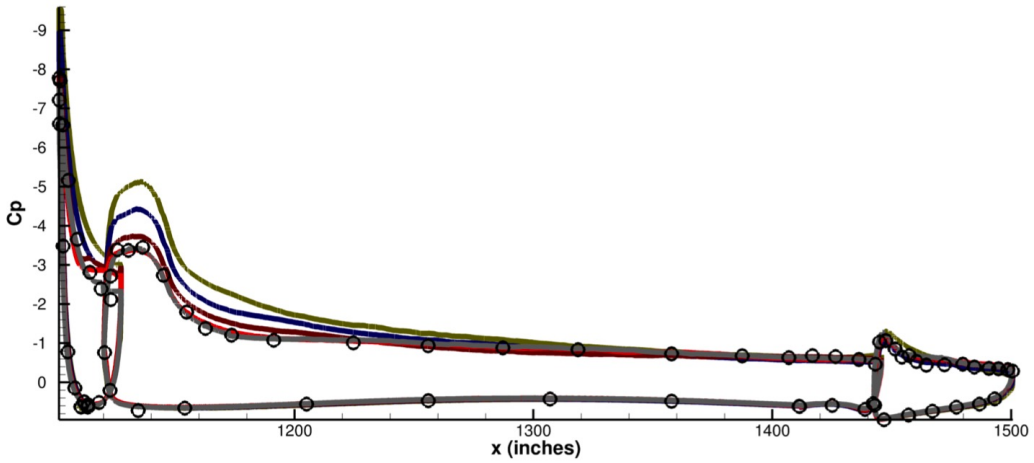
(c) 4mm Grid (1100M)

In-Tunnel Simulations – Cartesian IB-WMLES

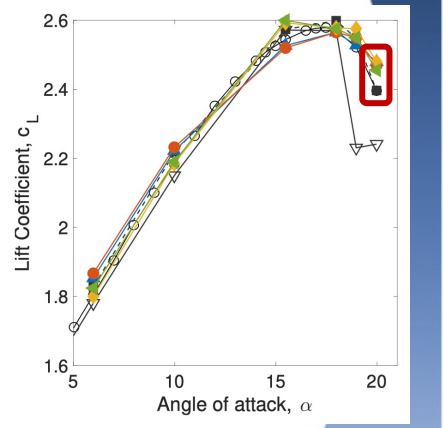
$\alpha = 19.98^{\circ}$ (Inboard sections)

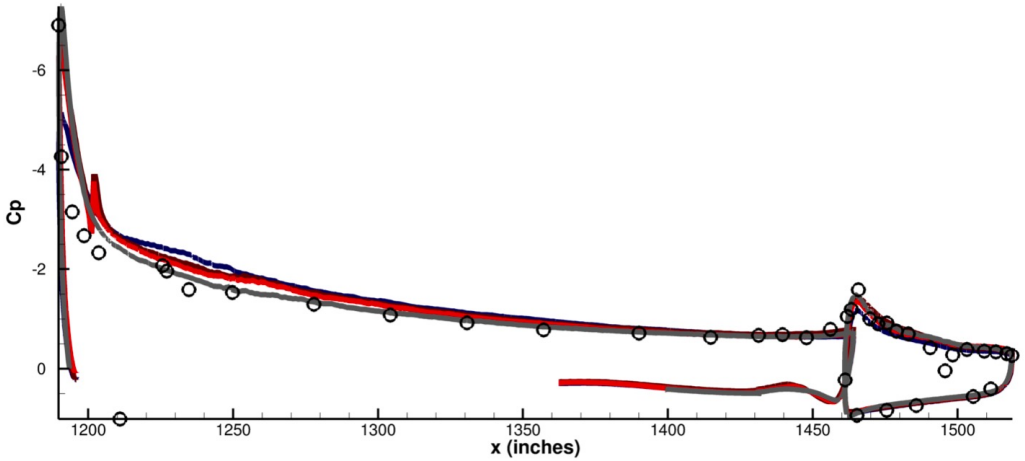


(a) Section A, $\eta = 0.15$

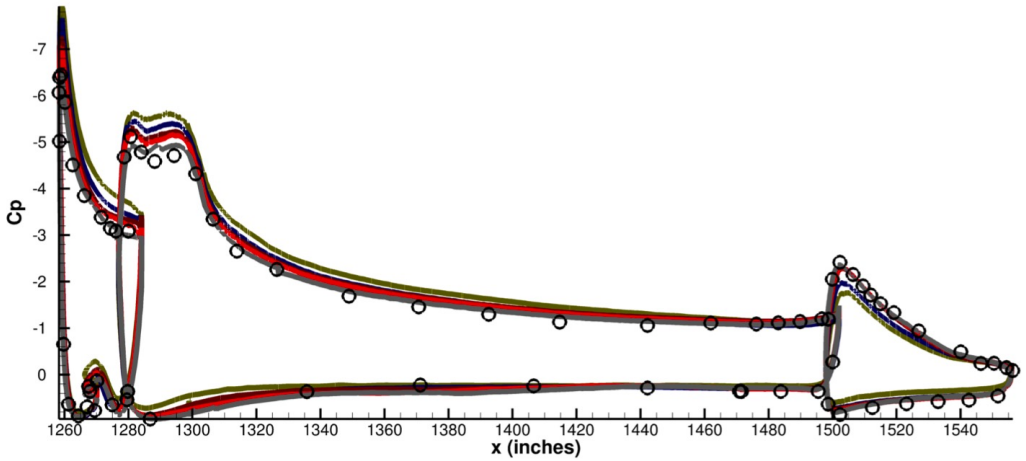


(b) Section B, $\eta = 0.24$

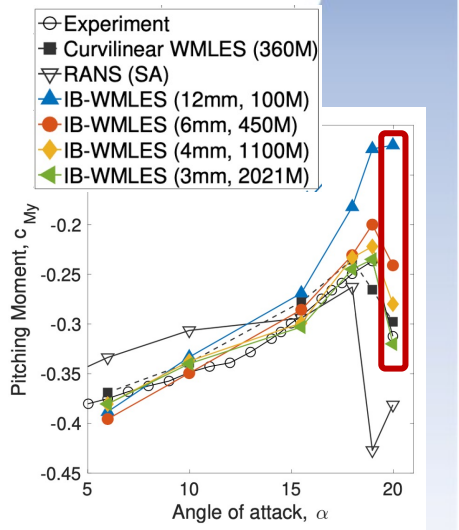




(c) Section C, $\eta = 0.24$

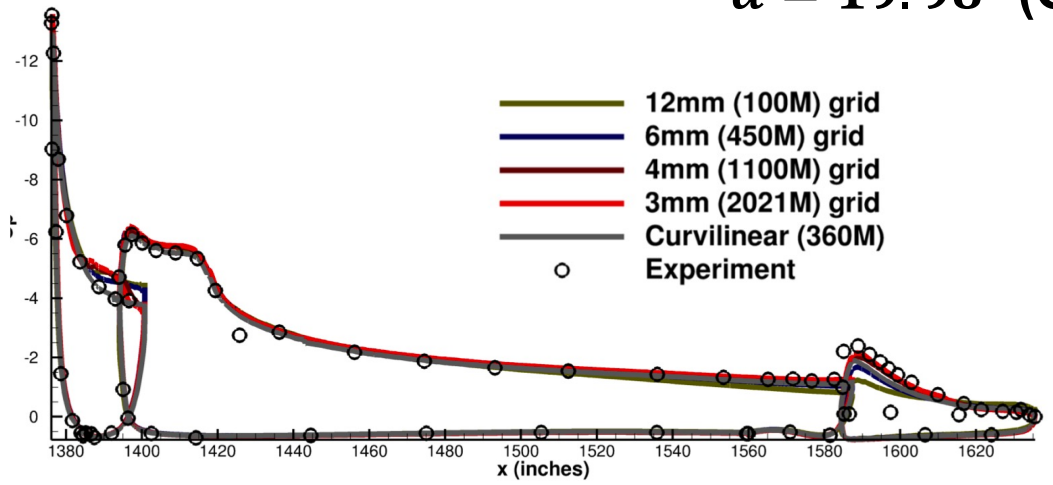


(d) Section D, $\eta = 0.33$

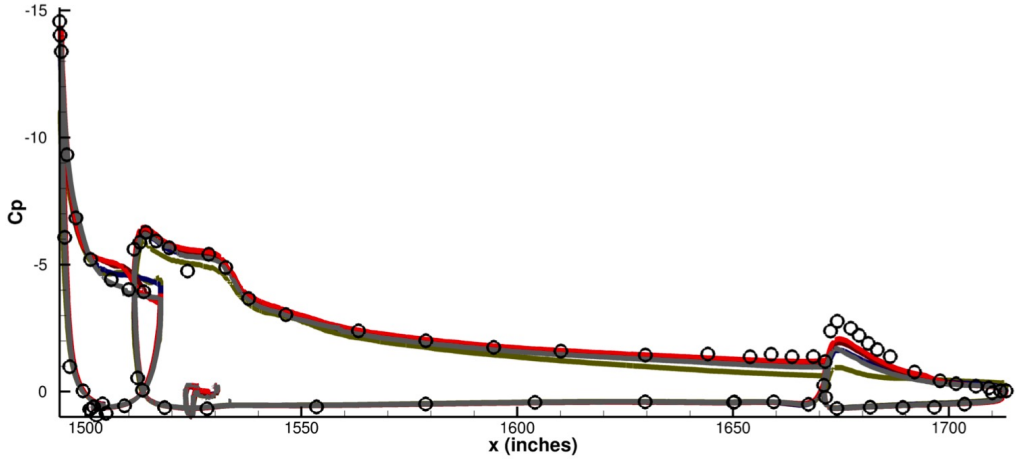


In-Tunnel Simulations – Cartesian IB-WMLES

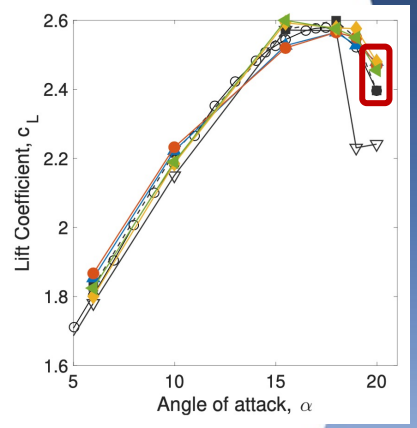
$\alpha = 19.98°$ (Outboard sections)

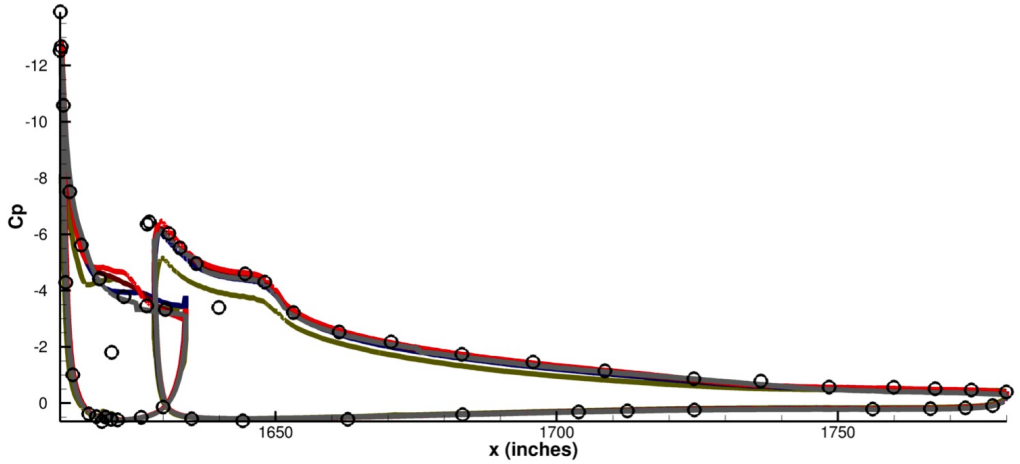


(e) Section E, $\eta = 0.55$

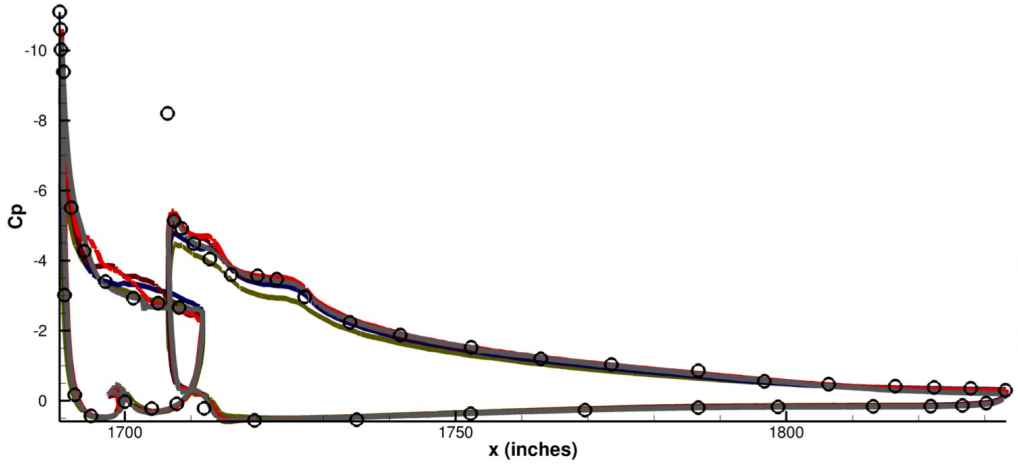


(f) Section F, $\eta = 0.69$

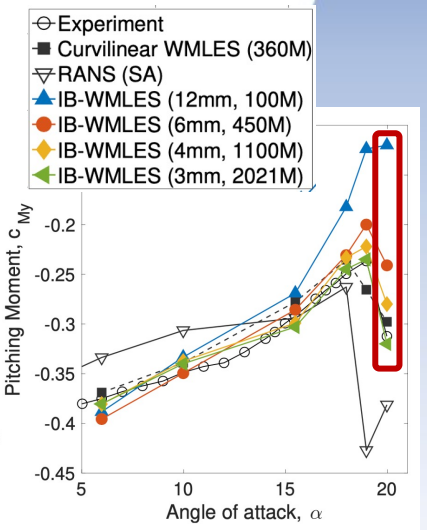




(g) Section G, $\eta = 0.82$

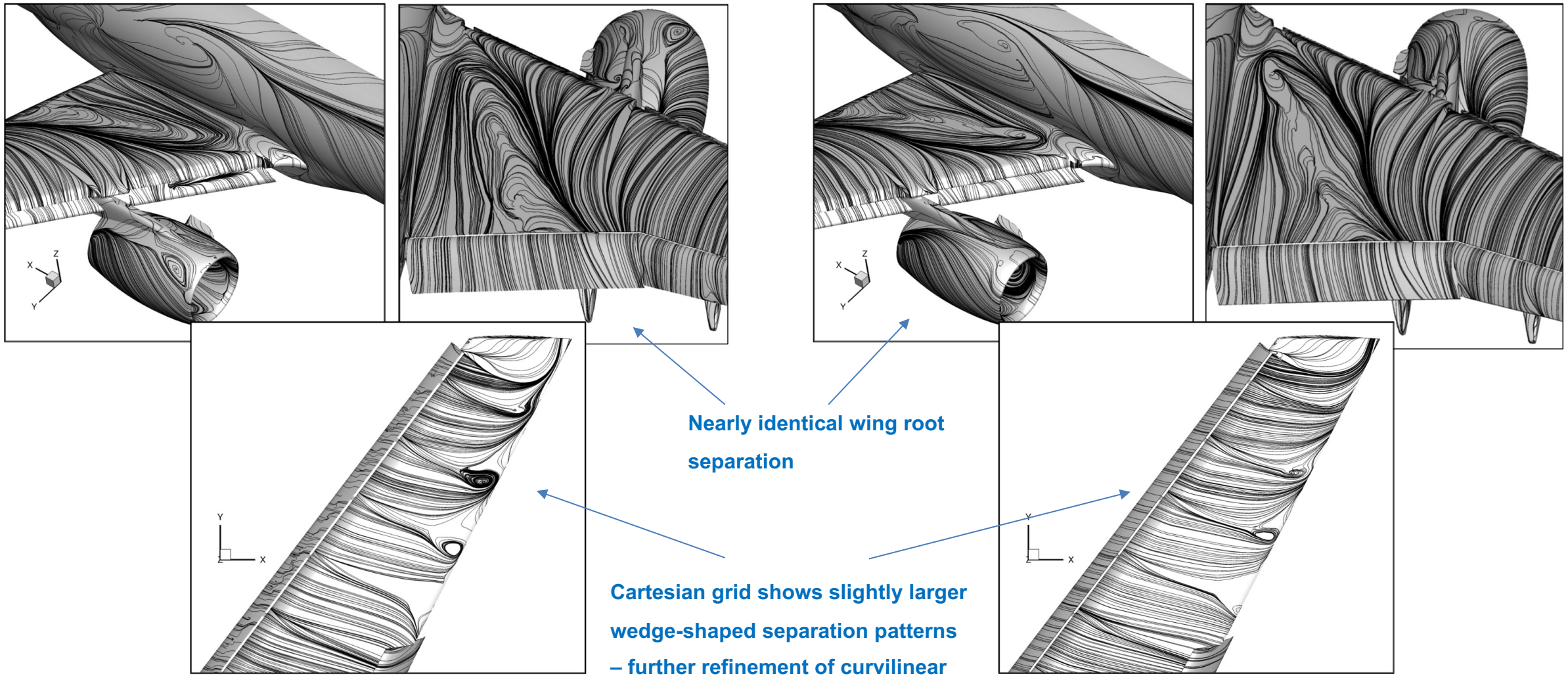


(h) Section H, $\eta = 0.91$



In-Tunnel Simulations

$$\alpha = 19.98^{\circ}$$



Nearly identical wing root separation

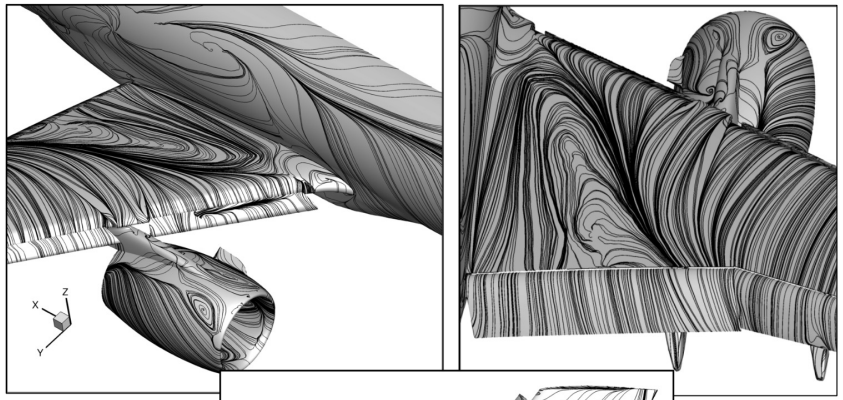
Cartesian grid shows slightly larger wedge-shaped separation patterns – further refinement of curvilinear grid leads to a similar increase

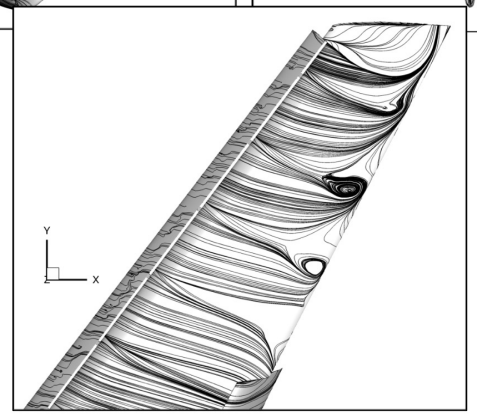
(a) Cartesian WMLES (3mm Grid)

(b) Curvilinear WMLES

In-Tunnel Simulations

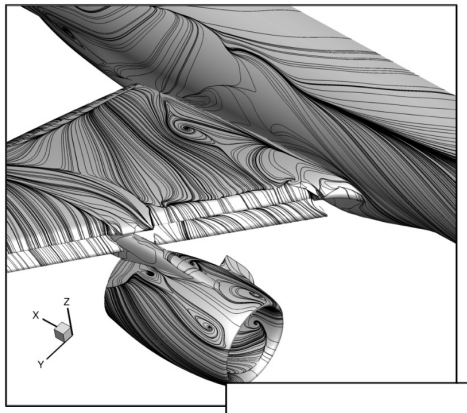
$\alpha = 19.98°$

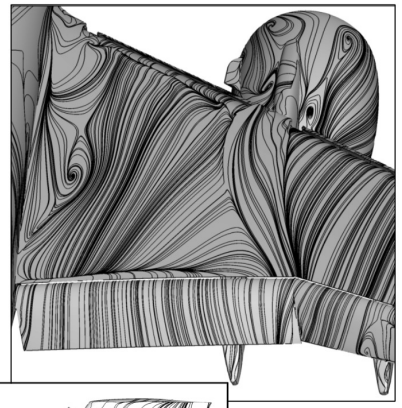


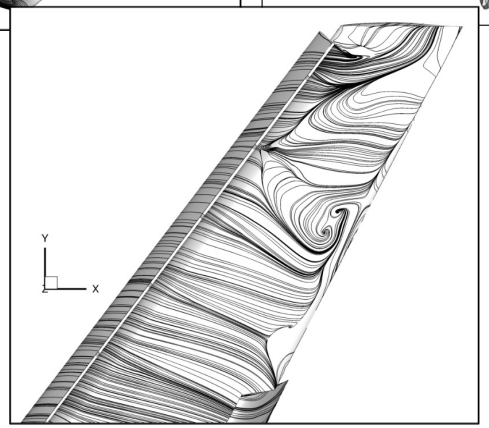


Cartesian WMLES

(Present Work)

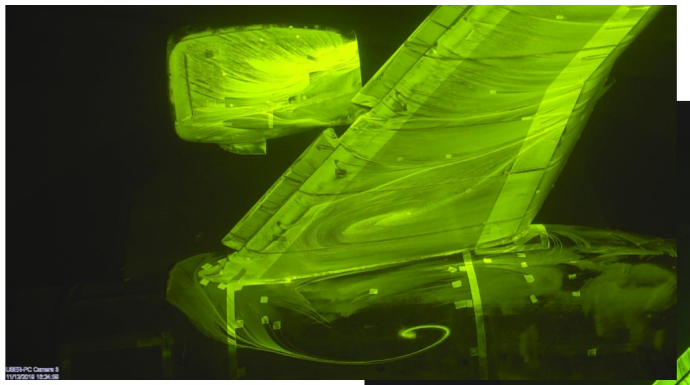


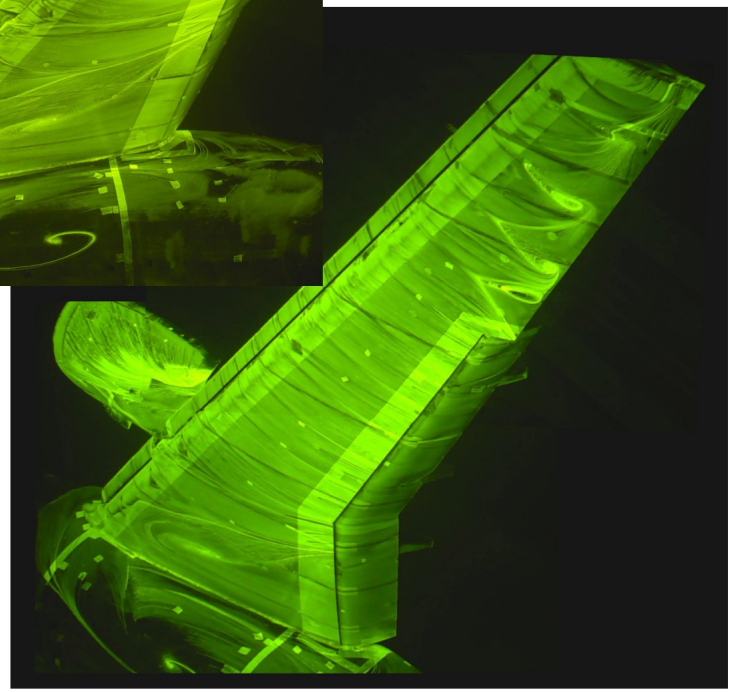




Steady-State RANS

(Duensing et al., 2022)



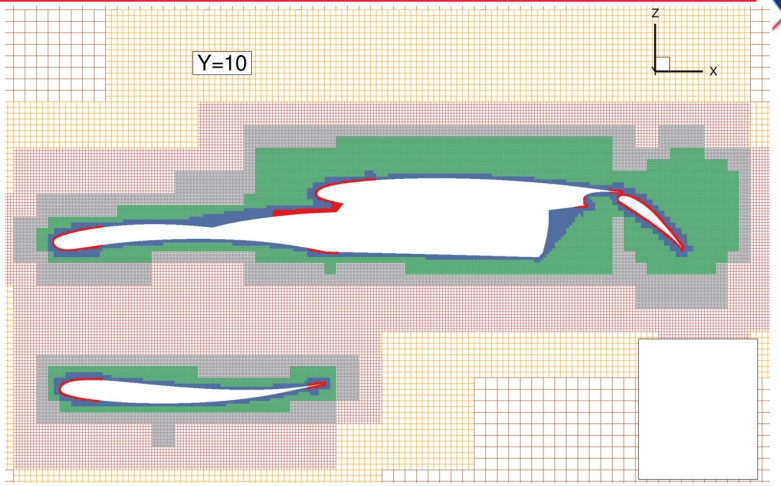


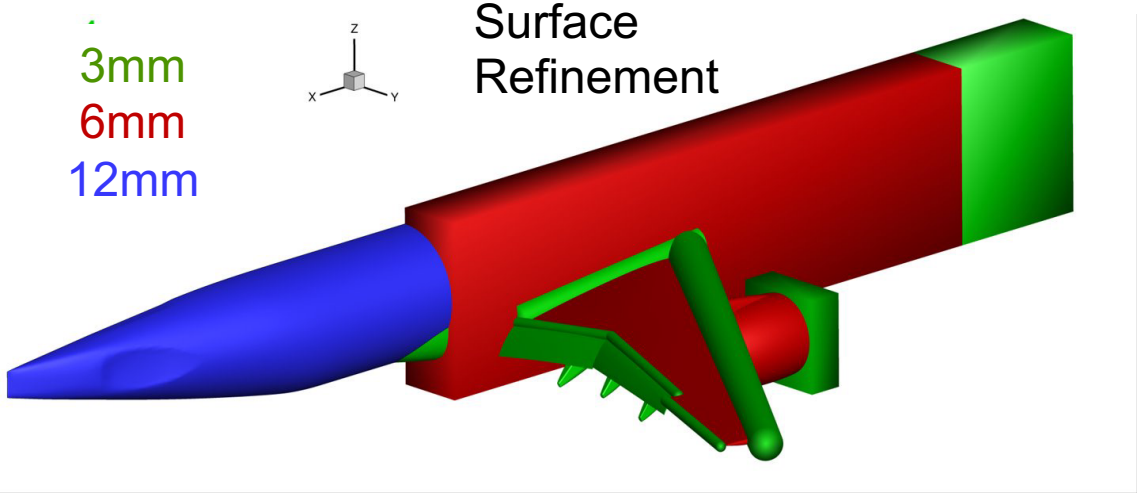
Oil-Flow Imagery

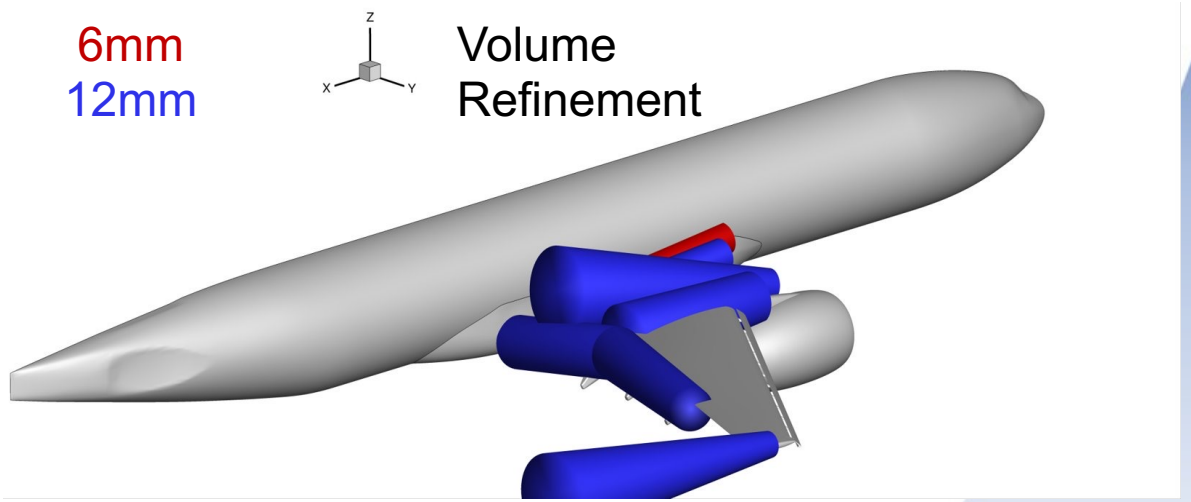
(HLPW4-Website)

In-Tunnel Simulations

- Further **2mm refined grid** (approx. 6B grid points) simulations underway to study convergence at $\alpha = 19.98°$
- Engineering "Best-practice" grid can be designed using **targeted refinement** sensitivities shown before





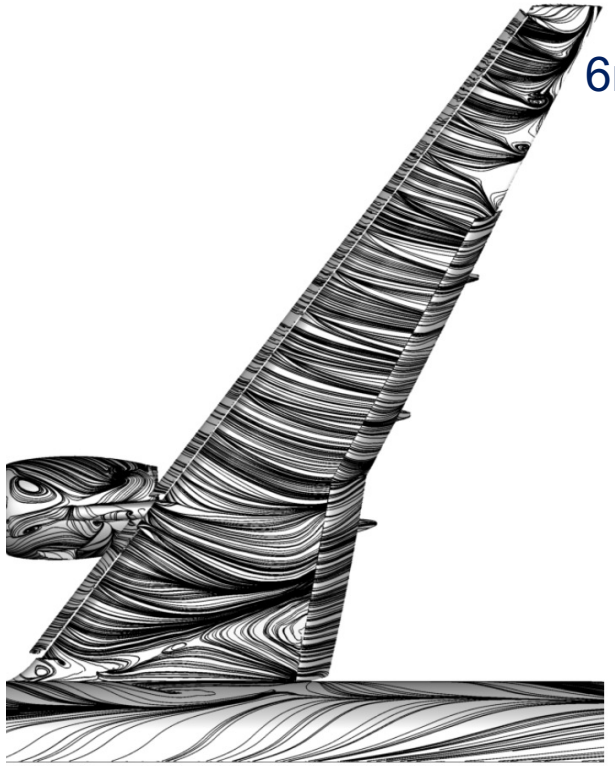


6mm grid (450M) → 3mm + 6mm grid (1000M)*

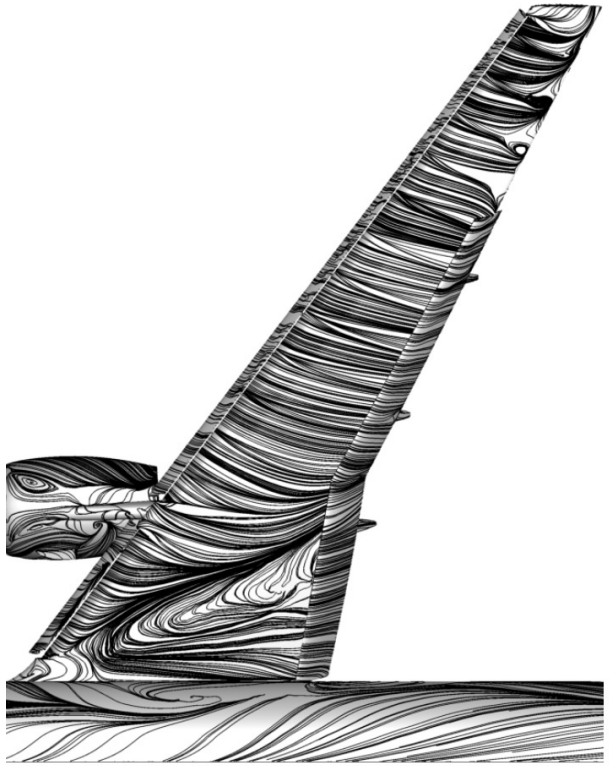
* Refinement blocks shown above are slightly different from the final refinement strategy that was used

In-Tunnel Simulations

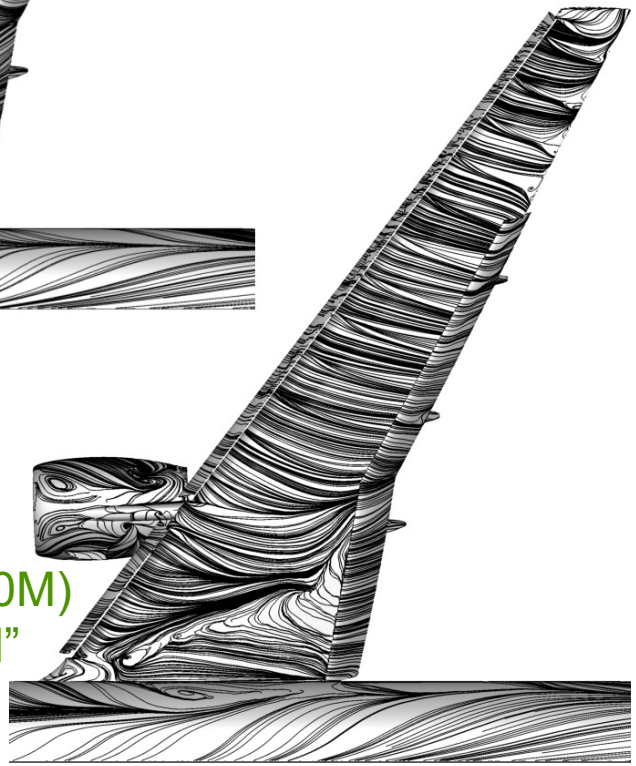
6mm (450M) grid

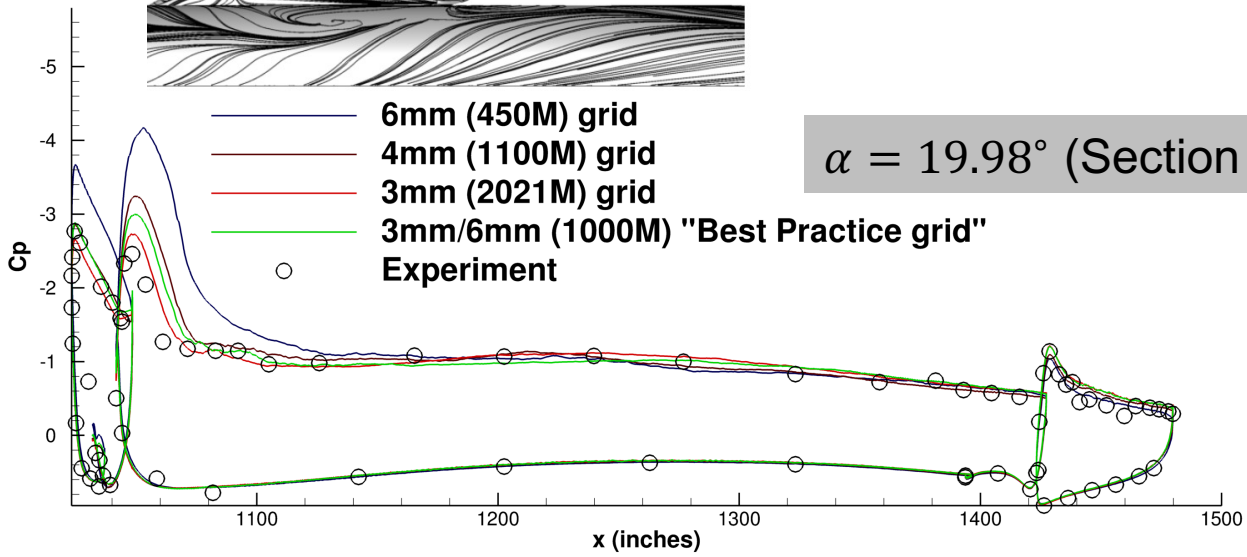


3mm (2021M) grid



3mm + 6mm (1000M)
“Best Practice grid”



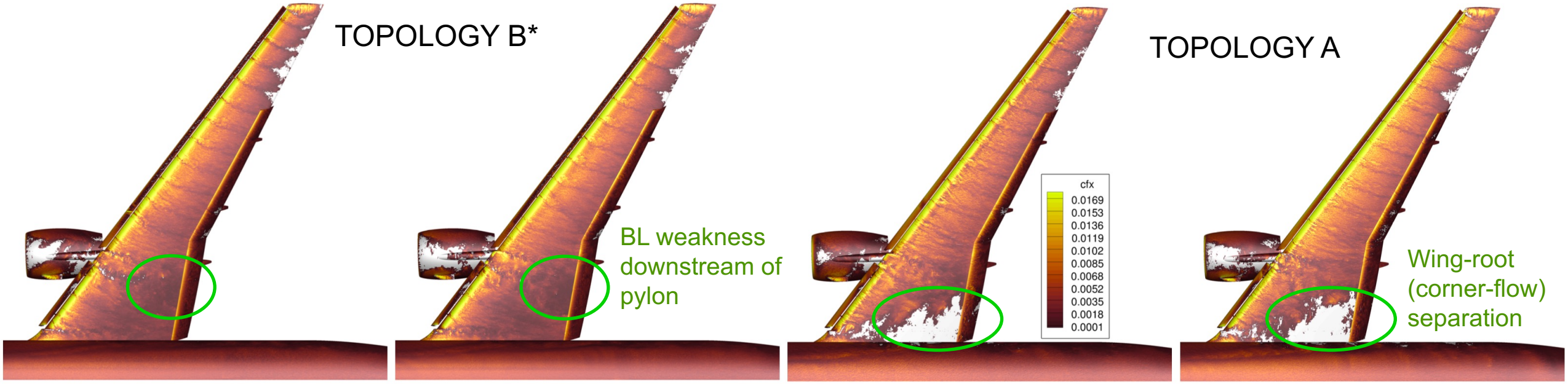


$\alpha = 19.98°$ (Section A)

Part B: Some Unexpected Results

Observation 1: Free-Air onset of stall

$\alpha = 21.47°$ (Corrected for Free-Air)



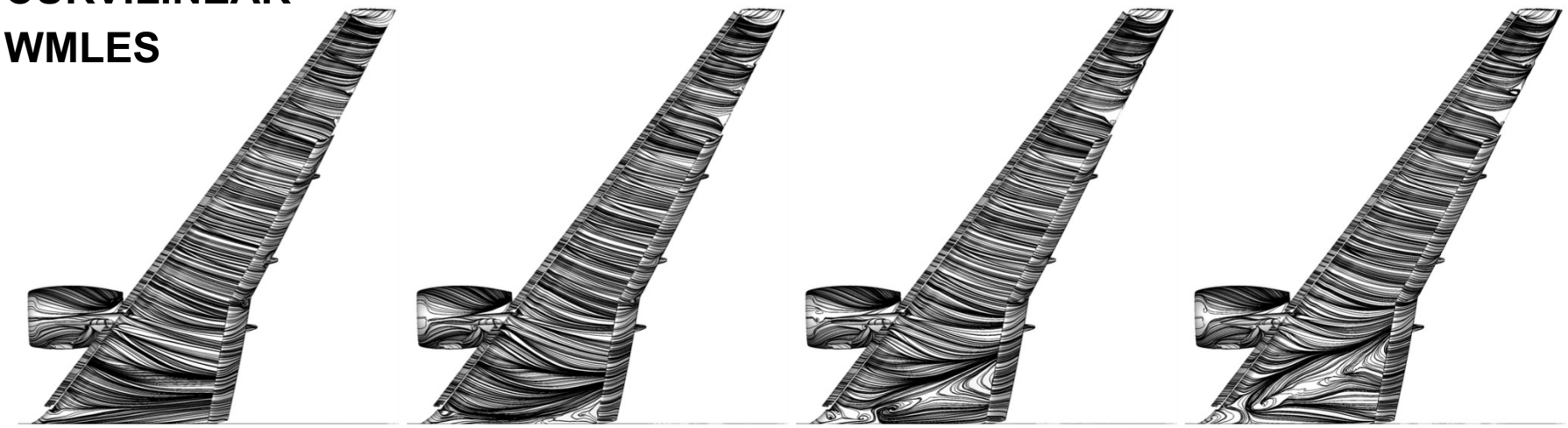
(a) Cartesian 4mm Grid (1100M) (b) Cartesian 3mm Grid (2021M) (c) Curvilinear Grid W-B (360M) (d) Curvilinear Grid W-D (1100M)

- Curvilinear and Cartesian grids seem to predict distinct post – CLmax flow topologies
- Both simulations show Nacelle-separation (see Lacy & Clark, 2021 for discussion on Nacelle-lip design)
- Cartesian does not predict a pitch break in free-air
- Curvilinear predicts a weak pitch break in free-air
- Both methods predict identical loads/surface flow topologies for $\alpha < 19.5°$

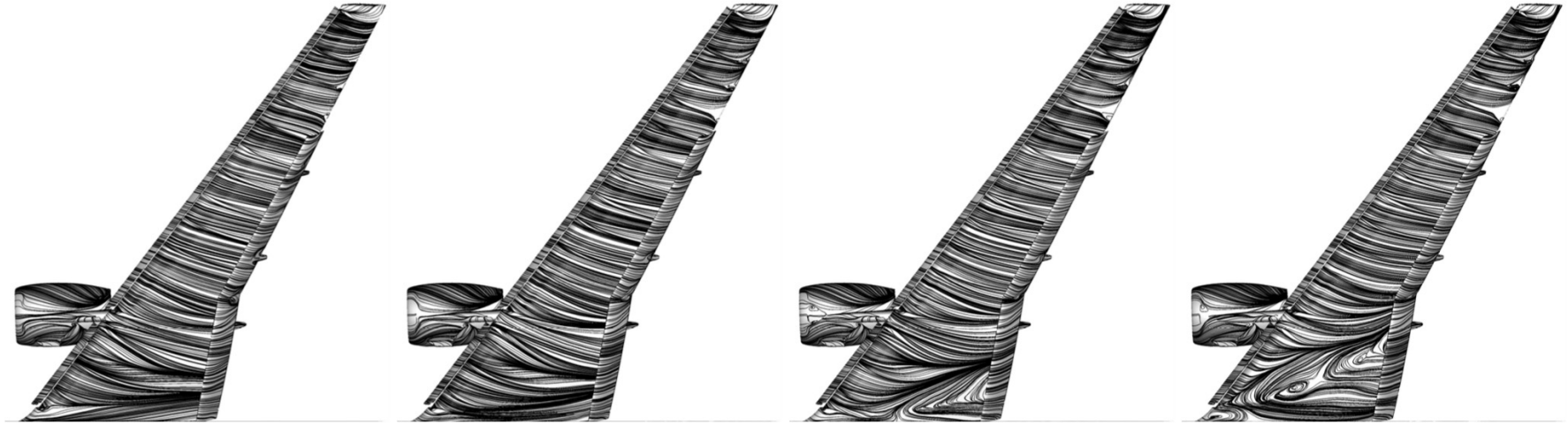
*First observed by Koneig et al. (using PowerFLOW) in 2021

Observation 2: Floor BL and In-tunnel onset of stall

CURVILINEAR WMLES



(a) $\alpha = 15.48°$, Viscous Tunnel (b) $\alpha = 17.98°$, Viscous Tunnel (c) $\alpha = 18.97°$, Viscous Tunnel (d) $\alpha = 19.98°$, Viscous Tunnel



(e) $\alpha = 15.48°$, Inviscid Tunnel (f) $\alpha = 17.98°$, Inviscid Tunnel (g) $\alpha = 18.97°$, Inviscid Tunnel (h) $\alpha = 19.98°$, Inviscid Tunnel

- Presence of floor BL results in earlier onset of wing-root separation (some consistency with experiments by Evans et al., 2020)
- Once large-scale separation occurs, no real sensitivity observed (occurrence of instability?)

Outstanding Questions

- **Question 1: Why do curvilinear and cartesian methods predict two distinct topologies in free-air? Is one of them (or both) incorrect?**
  - Lots of correlations between off-body vorticity and surface flow
  - No causal explanation determined as of this time
  - Several possibilities speculated in paper (Nacelle-separation + chine vortex, increasing CL branch vs decreasing CL branch, etc.)

- **Question 2: If the two methods disagree in free-air, why do they agree so well for in-tunnel simulations?**
  - Addressed next

- **Question 3: Why does the floor BL affect stall onset? Would it affect flap separation at low angles?**
  - Addressed next

Part C: Uncertainties with Free-Air corrections

Tunnel vs. Free-Air

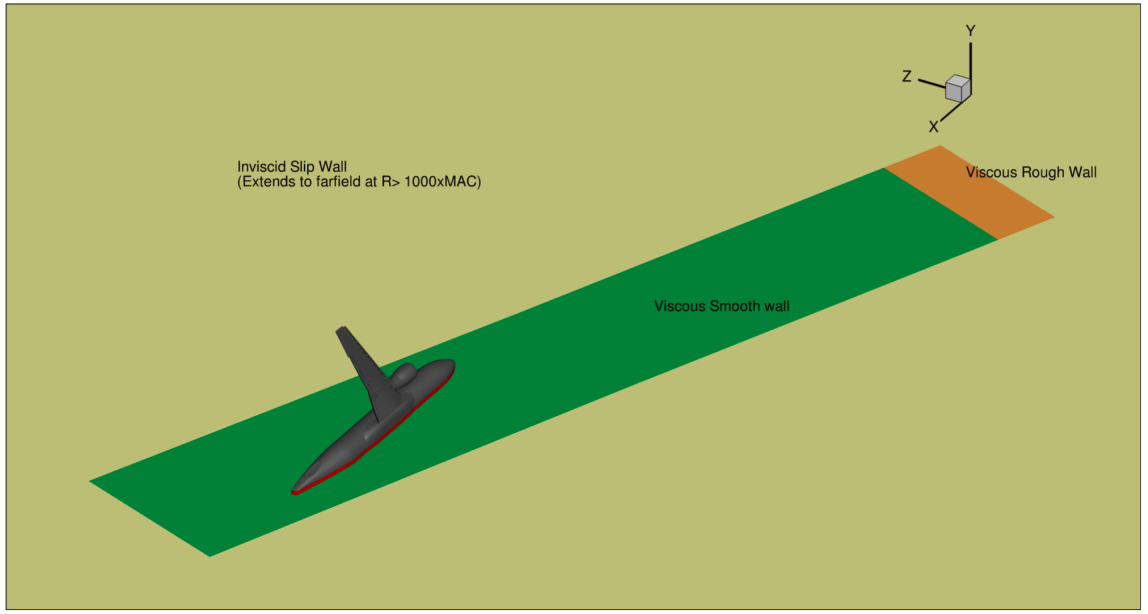
- **3 primary differences between the two environments:**
  - Blockage/Confinement effects: Will assume this gets correctly accounted for via the map

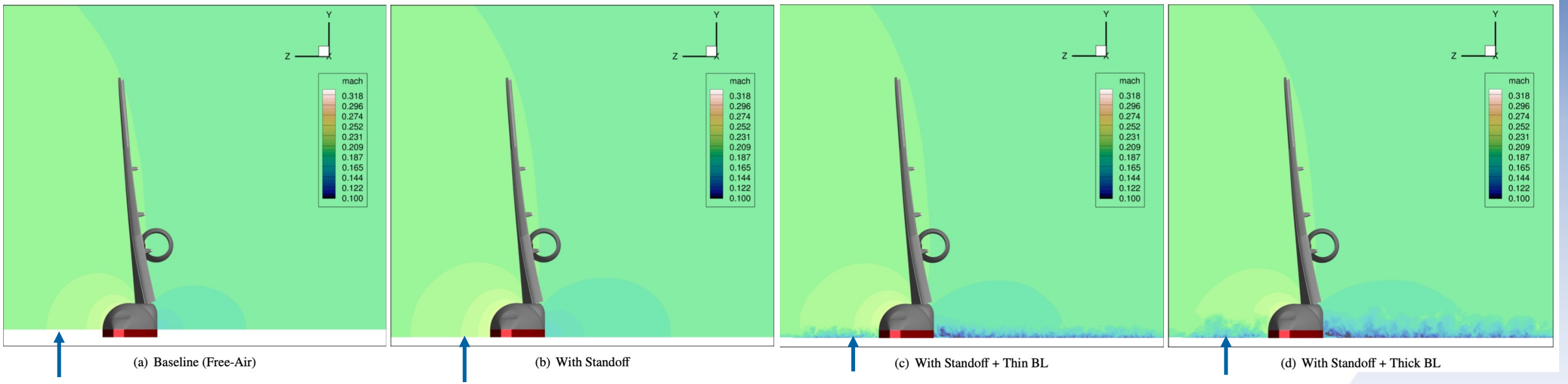
$$\{\alpha, C_L, C_D, C_{My}\} \rightarrow \{\alpha^{FA}, C_L^{FA}, C_D^{FA}, C_{My}^{FA}\}$$

  - Standoff/Peniche height: Unsure if it gets accounted for in corrections (Murayama et al, 2008; Yokokawa et al. 2010)
  - Tunnel Boundary layer: Unsure if it gets accounted for in corrections (Giguere et al., 1996; Rogers et al., 2000; Singh et al., 2019)

Standoff & Floor BL Effects

- Numerical experiments: 4 free-air (unconfined) simulations using Cartesian IB-WMLES (4mm, 1100M grid)
- Attempting to separate the blockage effects from tunnel wall/floor effects





(a) Baseline (Free-Air)

(b) With Standoff

(c) With Standoff + Thin BL

(d) With Standoff + Thick BL

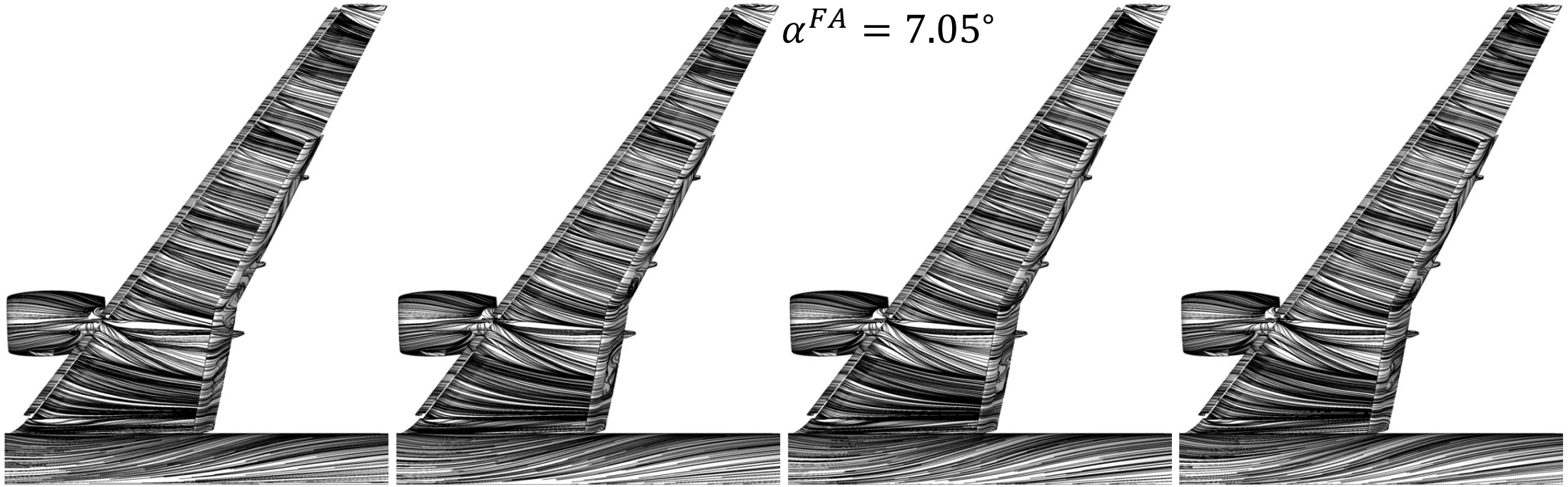
Symmetry plane (inviscid floor) at $y = 0m$

Symmetry plane (inviscid floor) at $y = -0.8m$

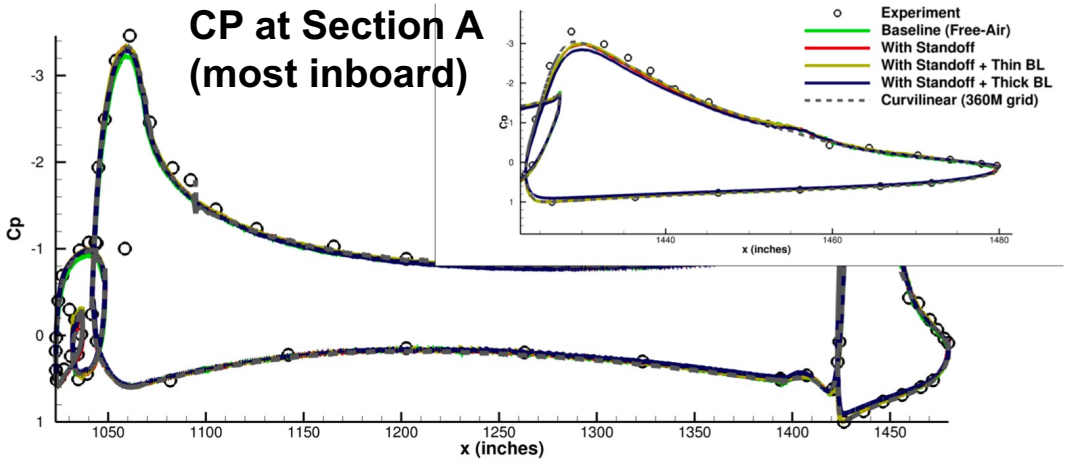
Floor BL at rake is approx. same as in-tunnel simulations

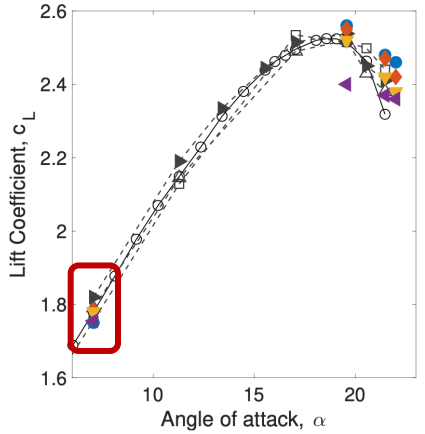
Floor BL at rake is approx. 75% thicker than in-tunnel experiments

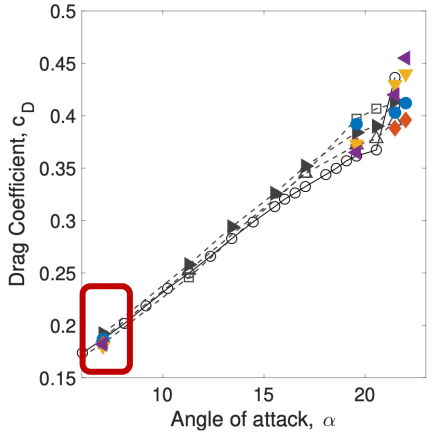
Standoff & Floor BL Effects

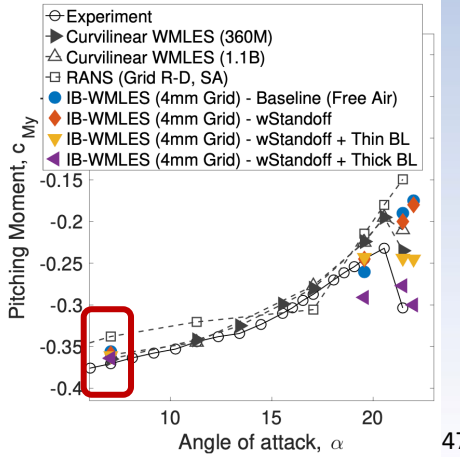


(a) Baseline (Free-Air) (b) With Standoff (c) With Standoff + Thin BL (d) With Standoff + Thick BL



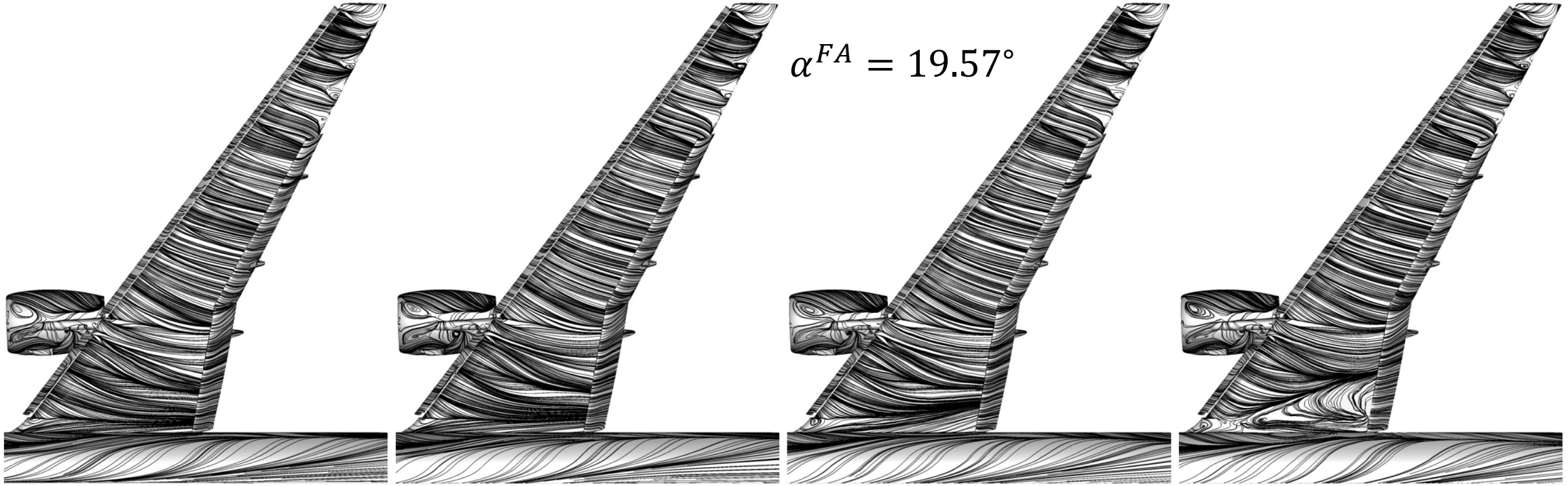




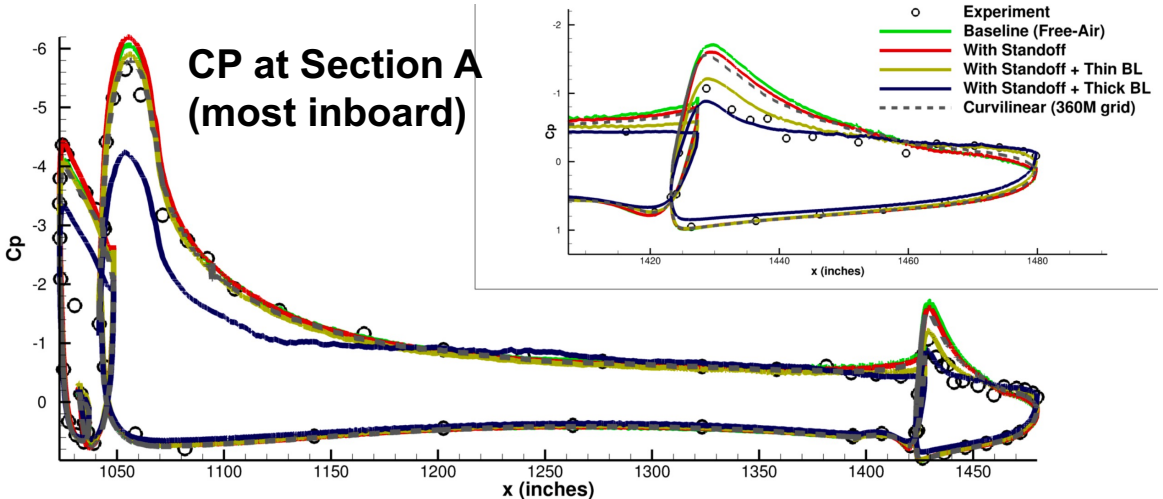


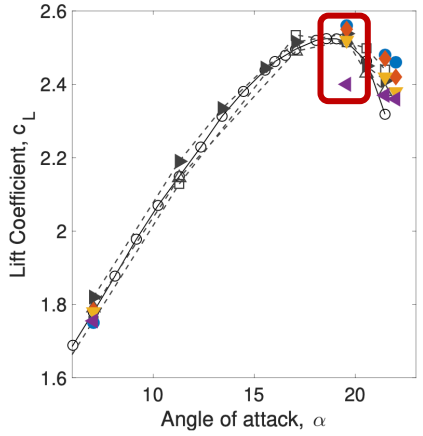
Standoff & Floor BL Effects

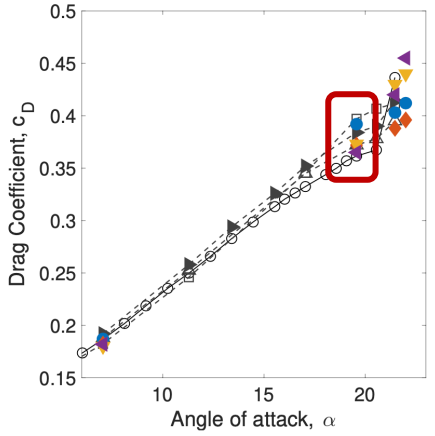
$\alpha^{FA} = 19.57°$

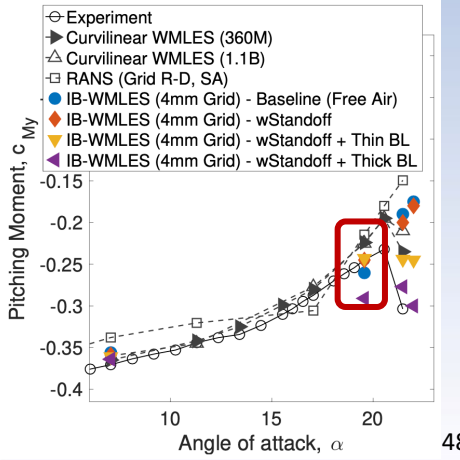


(a) Baseline (Free-Air) (b) With Standoff (c) With Standoff + Thin BL (d) With Standoff + Thick BL



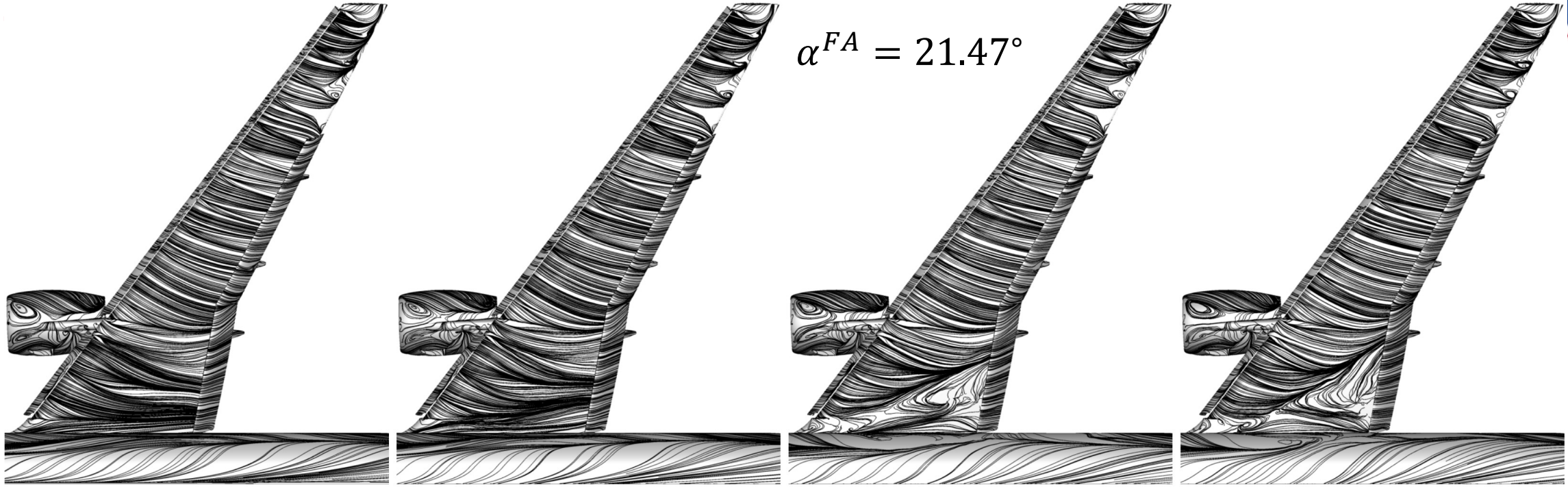




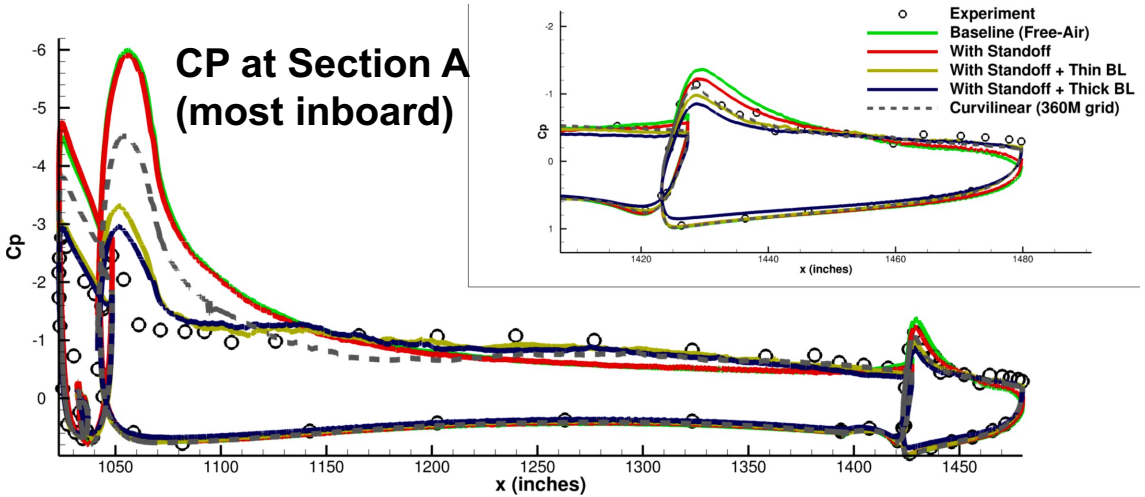


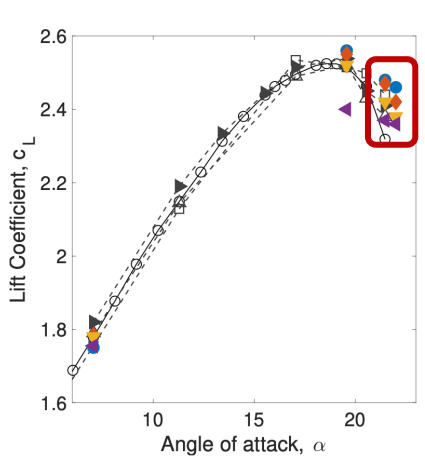
Standoff & Floor BL Effects

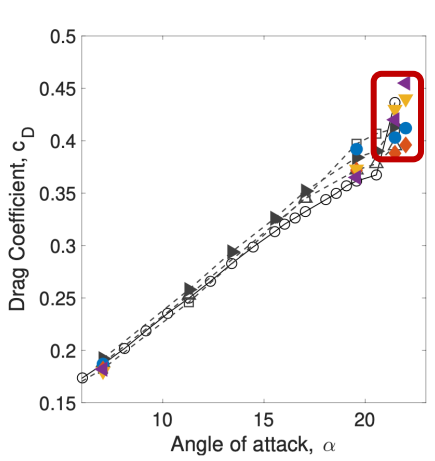
$\alpha^{FA} = 21.47°$

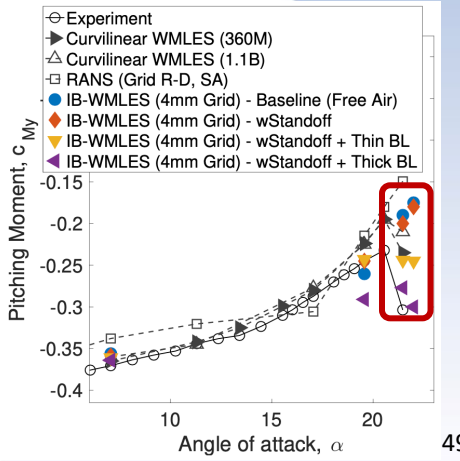


(a) Baseline (Free-Air) (b) With Standoff (c) With Standoff + Thin BL (d) With Standoff + Thick BL









Standoff & Floor BL Effects

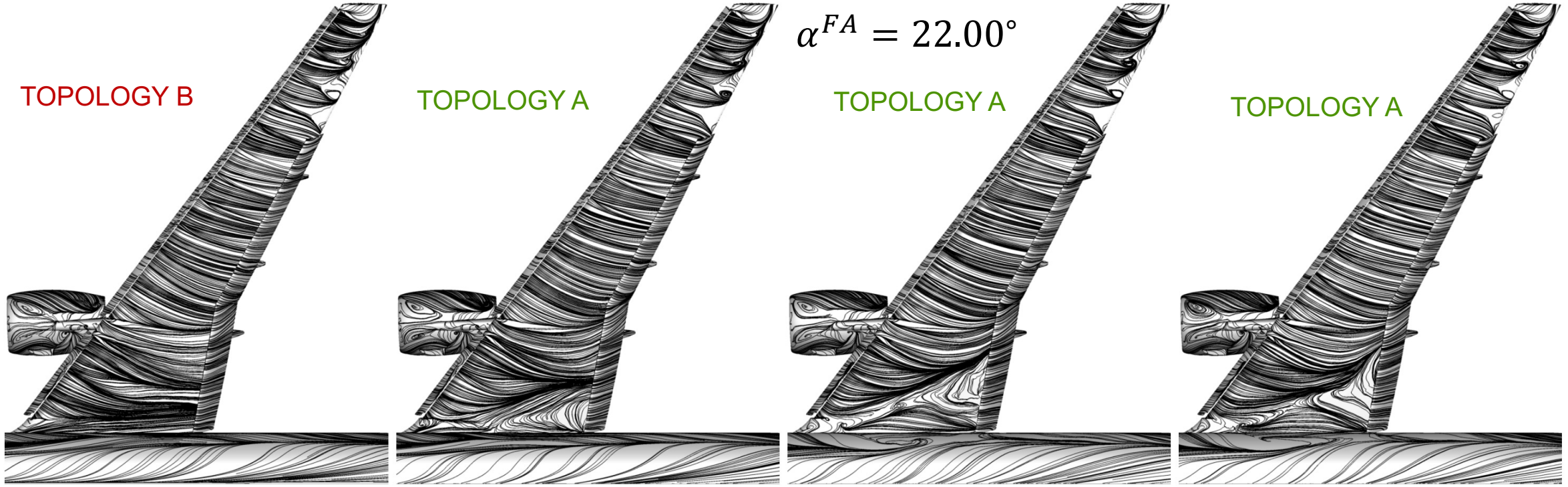
$\alpha^{FA} = 22.00°$

TOPOLOGY B

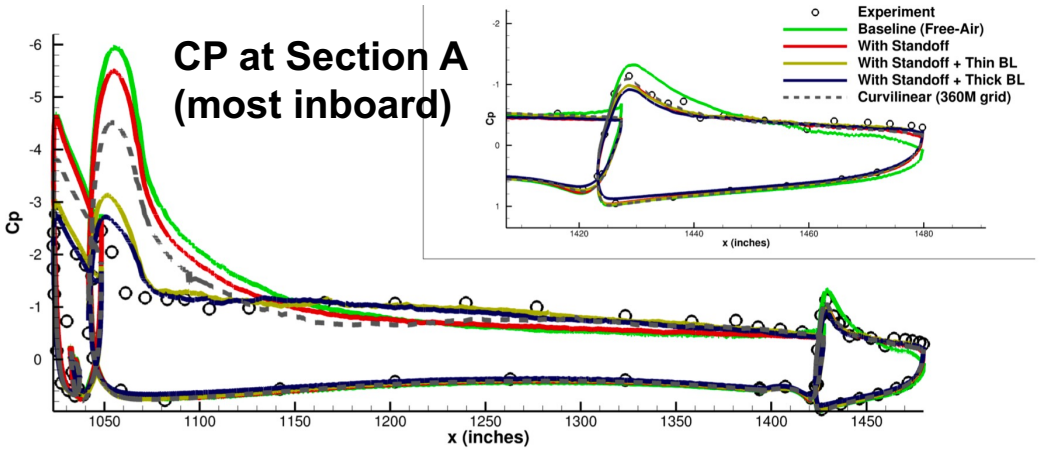
TOPOLOGY A

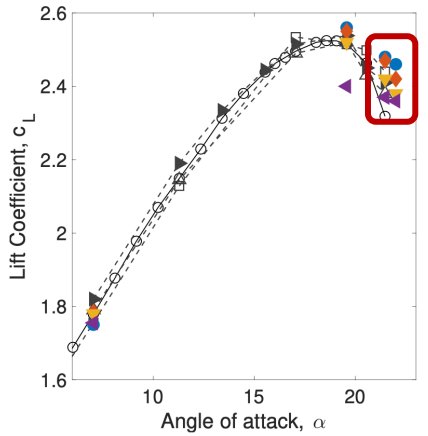
TOPOLOGY A

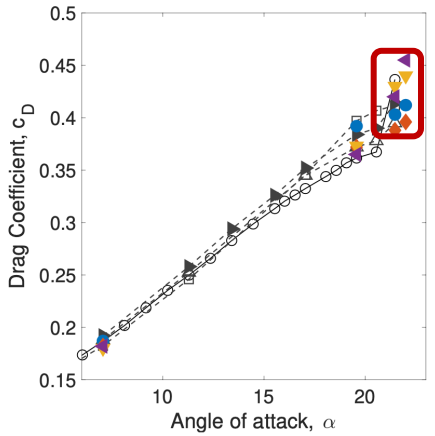
TOPOLOGY A

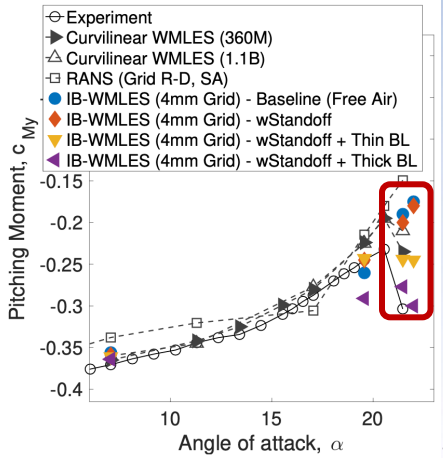


(a) Baseline (Free-Air) (b) With Standoff (c) With Standoff + Thin BL (d) With Standoff + Thick BL





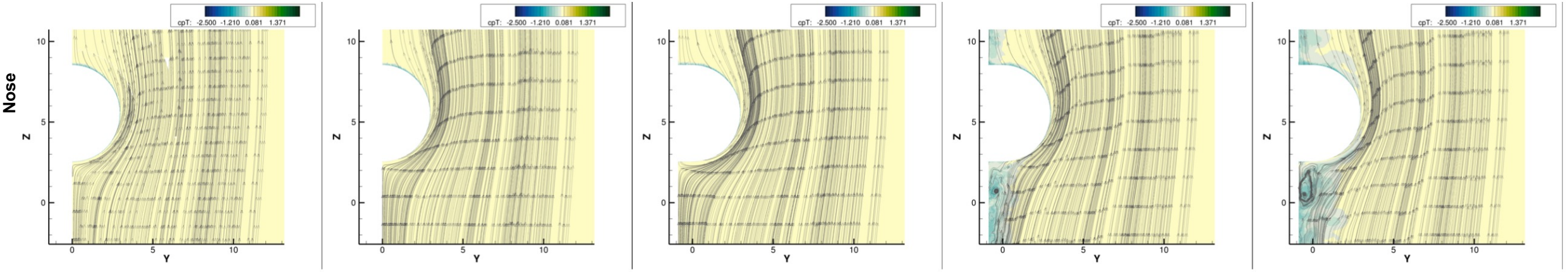




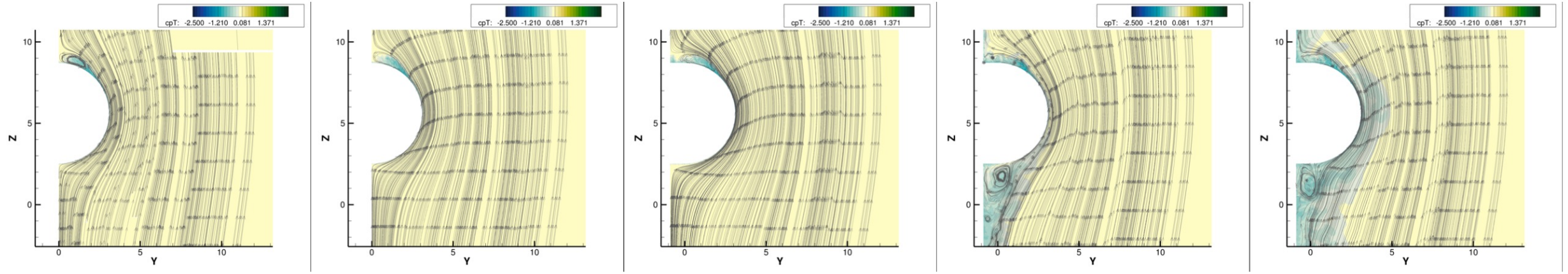
Standoff & Floor BL Effects

Stagnation pressure coefficient along **constant x planes** $\left(\alpha^{FA} = 19.57°\right)$

Fuse Nose



(a) Curv ($x = 10.14$m) (b) Base ($x = 10.14$m) (c) Stand ($x = 10.14$m) (d) ThinBL ($x = 10.14$m) (e) ThickBL ($x = 10.14$m)



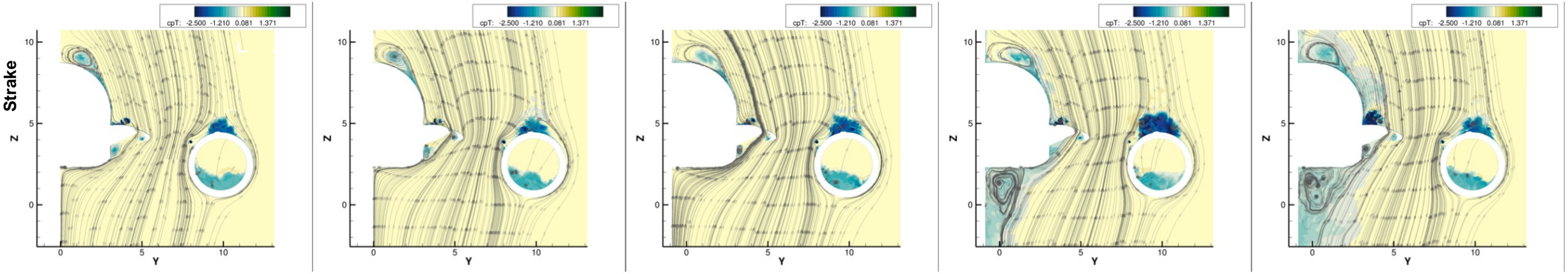
(f) Curv ($x = 20.44$m) (g) Base ($x = 20.44$m) (h) Stand ($x = 20.44$m) (i) ThinBL ($x = 20.44$m) (j) ThickBL ($x = 20.44$m)

Downstream Towards Wing

Standoff & Floor BL Effects

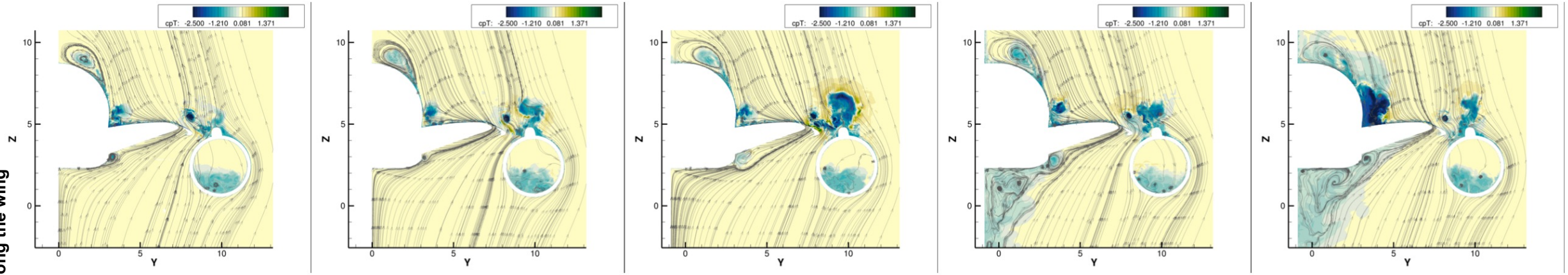
Stagnation pressure coefficient along **constant x planes** $\left(\alpha^{FA} = 19.57°\right)$

Wing LE Strake



(p) Curv ($x = 26.61$m) (q) Base ($x = 26.61$m) (r) Stand ($x = 26.61$m) (s) ThinBL ($x = 26.61$m) (t) ThickBL ($x = 26.61$m)

Downstream along the wing

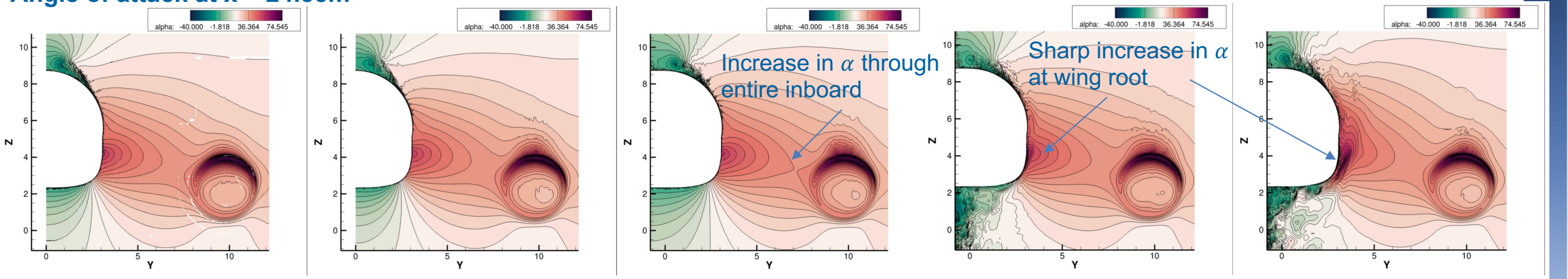


(u) Curv ($x = 28.67$m) (v) Base ($x = 28.67$m) (w) Stand ($x = 28.67$m) (x) ThinBL ($x = 28.67$m) (y) ThickBL ($x = 28.67$m)

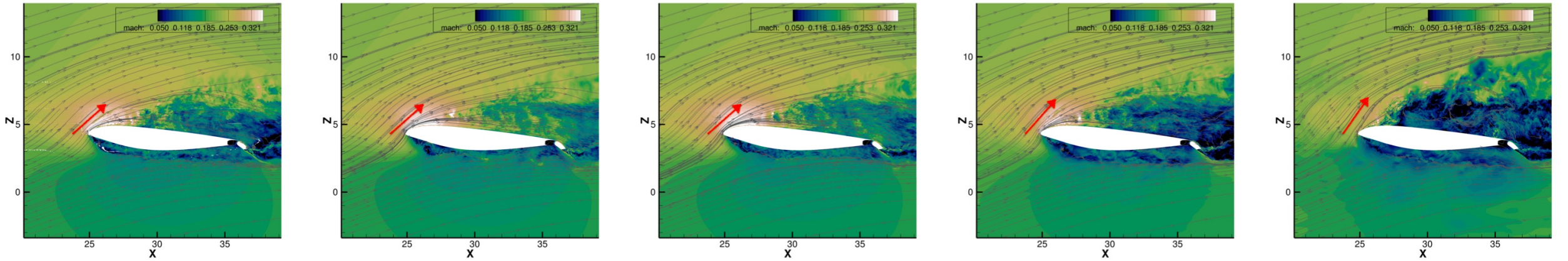
Standoff & Floor BL Effects

Effect on **apparent angle of attack** near **wing-root** $\left(\alpha^{FA} = 19.57°\right)$

Angle of attack at x = 24.55m



(a) Curv (b) Base (c) Stand (d) ThinBL (e) ThickBL



(a) Curv ($y = 3.15$m) (b) Base ($y = 3.15$m) (c) Stand ($y = 3.15$m) (d) ThinBL ($y = 3.15$m) (e) ThickBL ($y = 3.15$m)

Computational Costs for WMLES

Computational Costs for WMLES (on CPUs)

Attribute	Simulation Methodology				
	RANS (Steady) Grid R-C	Curv-WMLES Grid W-B	IB-WMLES 6mm, 450M grid	IB-WMLES 4mm, 1100M grid	IB-WMLES 3mm+6mm, 1000M BP grid
Solve Points	223M	360M	450M	1100M	2020M
Timestep size	-	$3.5\mu s$	$7.4\mu s$	$4.8\mu s$	$3.45\mu s$

Cartesian – Octree grids are larger for comparable near-wall resolutions

BUT …

Computational Costs for WMLES (on CPUs)

Attribute	Simulation Methodology				
	RANS (Steady) Grid R-C	Curv-WMLES Grid W-B	IB-WMLES 6mm, 450M grid	IB-WMLES 4mm, 1100M grid	IB-WMLES 3mm+6mm, 1000M BP grid
Solve Points	223M	360M	450M	1100M	2020M
Timestep size	-	$3.5\mu s$	$7.4\mu s$	$4.8\mu s$	$3.45\mu s$
Nodes used for benchmark	35 Skylakes (40 cores/node)	100 AMD Romes (128 cores/node)	100 Skylakes (40 cores/node)	100 Skylakes (40 cores/node)	100 Skylakes (40 cores/node)
Core-time per compute point per timestep	-	$2.03\mu s$	$0.75\mu s$	$0.75\mu s$	$0.75\mu s$

Cartesian – Octree grids are larger for comparable near-wall resolutions

BUT …

Cartesian WMLES is algorithmically much more efficient than curvilinear WMLES

Computational Costs for WMLES (on CPUs)

Attribute	Simulation Methodology				
	RANS (Steady) Grid R-C	Curv-WMLES Grid W-B	IB-WMLES 6mm, 450M grid	IB-WMLES 4mm, 1100M grid	IB-WMLES 3mm+6mm, 1000M BP grid
Solve Points	223M	360M	450M	1100M	2020M
Timestep size	-	$3.5\mu s$	$7.4\mu s$	$4.8\mu s$	$3.45\mu s$
Nodes used for benchmark	35 Skylakes (40 cores/node)	100 AMD Romes (128 cores/node)	100 Skylakes (40 cores/node)	100 Skylakes (40 cores/node)	100 Skylakes (40 cores/node)
Core-time per compute point per timestep	-	$2.03\mu s$	$0.75\mu s$	$0.75\mu s$	$0.75\mu s$
Timesteps per CTU	-	29,338	13,782	21,392	29,561
Core-time per CTU	-	5970 hours	1300 hours	4900 hours	6100 hours
Simulation time needed for $\alpha = 19.57°$	-	50 CTU	50 CTU	50 CTU	50 CTU
Core-time needed for $\alpha = 19.57°$	21,000 hours	298,500 hours	65,000 hours	245,000 hours	308,000 hours
NAS SBUs needed for $\alpha = 19.57°$	**835**	**9,470**	**2,600**	**9,800**	**12,240**
Relative Cost over typical RANS	**1.0**	**11.3**	**3.1**	**11.7**	**14.6**

Cartesian – Octree grids are larger for comparable near-wall resolutions

BUT …

Cartesian WMLES is algorithmically much more efficient than curvilinear WMLES

CRUNCHING THROUGH THE NUMBERS …

Both Curvilinear WMLES and Cartesian WMLES have similar accuracy/cost advantages over Steady-State RANS

HOWEVER …

Computational Costs for WMLES (on CPUs)

Attribute	Simulation Methodology				
	RANS (Steady) Grid R-C	Curv-WMLES Grid W-B	IB-WMLES 6mm, 450M grid	IB-WMLES 4mm, 1100M grid	IB-WMLES 3mm+6mm, 1000M BP grid
Solve Points	223M	360M	450M	1100M	2020M
Timestep size	-	$3.5\mu s$	$7.4\mu s$	$4.8\mu s$	$3.45\mu s$
Nodes used for benchmark	35 Skylakes (40 cores/node)	100 AMD Romes (128 cores/node)	100 Skylakes (40 cores/node)	100 Skylakes (40 cores/node)	100 Skylakes (40 cores/node)
Core-time per compute point per timestep	-	$2.03\mu s$	$0.75\mu s$	$0.75\mu s$	$0.75\mu s$
Timesteps per CTU	-	29,338	13,782	21,392	29,561
Core-time per CTU	-	5970 hours	1300 hours	4900 hours	6100 hours
Simulation time needed for $\alpha = 19.57°$	-	50 CTU	50 CTU	50 CTU	50 CTU
Core-time needed for $\alpha = 19.57°$	21,000 hours	298,500 hours	65,000 hours	245,000 hours	308,000 hours
NAS SBUs needed for $\alpha = 19.57°$	**835**	**9,470**	**2,600**	**9,800**	**12,240**
Relative Cost over typical RANS	**1.0**	**11.3**	**3.1**	**11.7**	**14.6**
Grid Generation (Human Effort)	**2-3 months**	**2-3 months**	**2-3 hours**	**2-3 hours**	**2-3 hours**

Cartesian – Octree grids are larger for comparable near-wall resolutions

BUT …

Cartesian WMLES is algorithmically much more efficient than curvilinear WMLES

CRUNCHING THROUGH THE NUMBERS …

Both Curvilinear WMLES and Cartesian WMLES have similar accuracy/cost advantages over Steady-State RANS

HOWEVER …

Cartesian WMLES requires the least amount of prep time by an overwhelming margin

Computational Costs for WMLES – Outlook (GPU acceleration)

- **All but 2 of the top 15 systems have GPU accelerators**
- GPU variant of the LAVA WMLES code uses **CUDA Fortran;** retains much of the same structure as the CPU code
- Relevant metrics (benchmark includes 66% of runtime of typical WMLES cases):
  - MUPS: Millions of UPdates (timesteps) per Second → Higher is better
  - **MUPS/W: MUPS per unit Power** → Higher is better
- **A100 has 4.4X higher power efficiency than Skylake and 3.3X higher than Rome**
- Significant fraction of peak FLOPS on all CPUs/GPUs **→ All implementations are well optimized**

Architecture	Type	MUPS	Power, TDP (W)	MUPS/ W	Theoretical Peak DP Flops (TF)	Estimated Fraction of Configured Peak Achieved (%)
2x Intel Skylake 6148 (AVX512)	CPU	78	300	0.26	3.1	21
2x AMD Rome 7742 (AVX2)	CPU	157	450	0.35	4.6	30
1x Nvidia V100 (CUDA)	GPU	330	300	**1.1**	7.5	**37**
1x Nvidia A100 (CUDA)	GPU	**461**	400	**1.15**	9.7	**40**

Summary

Summary

- Systematic study of consistent grid refinement performed using Cartesian Immersed Boundary WMLES for in-tunnel configuration:
  - For $\alpha < 18°$, largest source of resolution error seems to be outboard main-element and outboard flap; at least 6mm resolution needed to get the correct topology
  - For $\alpha > 18°$, largest source of resolution error seems to be near wing-root; coarser grids experience see the same topology but at higher angles (incipient separation moves to higher α)
  - Study highlights the potential for targeted refinements to achieve high accuracy per unit computational cost

- Free-Air simulations performed using curvilinear and cartesian WMLES yielded two distinct topologies for $\alpha^{FA} > 20°$ - this is worrying

Summary

- Numerical experiments to systematic differences between in-tunnel and free-air conducted:
  - Presence of the model standoff alters the angle of attack seen by the wing – effect decays with increasing distance from the symmetry plane (decays outboard) - this promotes onset of wing-root separation
  - Occurrence of a horseshoe-type vortex (prominently seen on the belly-side of the fuselage) due to viscous corner-flow interactions between model standoff and floor
  - Vortex leads to intense increase in angle of attack at the wing root – promoting onset of inboard separation
  - Observations also help explain the weak pitch-break seen in curvilinear free-air simulations; but good agreement seen for in-tunnel simulations

Summary

- Both Curvilinear and Cartesian WMLES seem to predict very accurate flow-topologies and integrated loads compared to the Qinetiq experiments; however, further refinement is needed for conclusive assessment
- Cartesian WMLES has significant advantages over Curvilinear WMLES:
  1. Orders of magnitude reduction in human effort for grid generation (months to hours)
  2. New immersed boundary formulation ensures comparable accuracy with body-fitted curvilinear formulation for a given Δ_x/δ_{BL}
  3. Facilitates very easy consistent grid refinement to be performed to understand sensitivities
  4. Easy to perform targeted (localized) refinement to optimize accuracy given a fixed computational cost

Acknowledgements

- Research funded by ARMD T^3 project under an RCA task
- Computational Resources provided by NASA Advanced Supercomputing on Aitken/Electra and Amazon Web Services (AWS)
- HLPW4 Organizers: Chris Rumsey, Jeff Slotnick and Caroline Woeber
- Interactions with WMLES TGF participants led to the floor-related numerical experiments; special thanks to Chris Rumsey and Benedikt Koenig
- Jeffrey Housman, Oliver Browne, Emre Sozer, Man Long Wong and other LAVA members for many fruitful discussions and development of post-processing tools



Iso-surfaces of Q-criterion
$\alpha = 19.98°$, Cartesian WMLES
3mm, 2010M point mesh
Video Credit: Timothy Sandstrom

Thank you for your attention!

LAVA Members that contributed to HLPW4:
Oliver Browne
Jared Duensing
Luis dos Santos Fernandes
Aditya Ghate
Jeffrey Housman
Cetin Kiris
Gaetan Kenway
Leonardo Machado
Elisha Makarevich
Daniel Maldonado
Gerrit-Daniel Stich